UNIVERSITAT POLITÈCNICA DE CATALUNYA
BARCELONATECH
Escola d'Enginyeria de Barcelona Est

FINAL BACHELOR'S DEGREE PROJECT

Bachelor of Mechanical Engineering

HIGH RESOLUTION GPR 3D IMAGES OPTIMIZATION

Memory and Annexes

Author: Arnaldo Vera Gonzalez
Director: María de la Vega Perez

Convocation: May 2017

Abstract

The present final bachelor's degree project is an experimental-based work, where we seek the optimization on the creation and representation of three dimensional images using ground penetrating radar (GPR) technology. This work investigates both the processing part and the most efficient way to obtain the data. The data processing was mainly performed with the software GPR-SLICE, although ReflexW was also used. Acquirement of data has been outdoors, specifically at EEBE school yard and at Forum beach in Barcelona, Spain.

Resum

Aquest treball de fi de grau és un treball d'investigació basat en l'experimentació pràctica, on es busca l'optimització en la creació i representació d'imatges en tres dimensions utilitzant la tecnologia de georadar o *groud penetrating radar* (GPR) en anglés. El treball indaga tant en el procesament informatic de les dades, com en la manera més eficient d'obtenció de les mateixes. El procesament de dades està fet principalment amb el programa GPR-SLICE, tot i que també s'ha utilitzat ReflexW. L'obtenció de dades ha tingut lloc a l'exterior, concretament al pati de l'escola EEBE i a la platja del Forum de Barcelona, Espanya.

Resumen

Este trabajo de fin de grado es un trabajo de investigación basado en la experimentación páctica, donde se busca la optimización en la creación y representación de imágenes en tres dimensiones utilizando la tecnología de georadar o *groud penetrating radar* (GPR), en inglés.El trabajo indaga tanto en el procesado informático de los datos, como en la manera más eficiete de obtener dichos datos. El procesado informático está hecho principalmente con el programa GPR-SLICE, aunque también se ha utilizado ReflexW. La obtención de los datos ha tenido lugar en exteriores, concretamente en el patio de la escuela EEBE y la playa del Forum de Barcelona, España.

Acknowledgements

I want to truly thank Vega Perez for so much patience, dedication and help. Saturday and Sunday phone calls, meetings on the middle of her exams, the books lent and lot of other details are so much appreciated and she is a huge part of this project.

As well I want to thank Viviana Sosa, who helped me a lot with the field work and processing time. We worked for hours for each field data acquirement, but without help, it would last days.

I will also want to thank my parents and my grandmother for so much patience and love brought to me from the first day of class to the last dot of this project. Those coffees/teas at the evenings gave me life. This project is for them.

Table of contents

Equations Index

Figure Index

Preface

This project will be pointing to the resolution and the most important topic and also to the correct software analysis using GPR-Slice. We will work with simple shapes of the objects that we burry, in order to set a general base for future projects and avoid approach to specific shapes/materials that may help less projects.

Roots of the project

The origin of this work came from my director Vega Perez, who is studying GPR technology for more than 18 years. She proposed me three possible projects related to GPR and I chose this one for being the most interesting from my point of view. Mostly for being a project of optimization and a project for looking for the best solutions giving certain conditions which is something that I enjoy to do.

Motivation

For this project, the main motivation is to be a tool for the upcoming projects. To be a guide and a base for continuing the study of vertical and horizontal resolution, as well as dense grid surveys for 3D imaging of GPR, and hopefully, provide a little contribution for the whole GPR world.

Introduction

The Ground Penetrating Radar (GPR) technology as we know it today, is relatively new and has been reaching new limits since it 1985 when the first commercial GPR systems arrived to the market. As this tool is only

We are going to bury various objects in different depths, each having different shape, dimensions and materials. Then, using the GPR equipment, we are going to take measures each centimeter around the buried object in order to obtain data for its study. With this raw data and using the software GPR-SLICE, we will process it and obtain a 3D image of each one, with the best resolution possible. This software will allow us to select the measures that the GPR had taken, that is, that we can select if we process data each centimeter, each two centimeters, three or whatever distance we decide.

Objectives

The main objective of this project is to be useful to others when it comes to the 3D representation from GPR radargrams. The way we are getting to this goal is by experimenting different controlled situations and then process the data by several processing methods in order to obtain substantial outcomes to perform better 3D images.

1. Brief historical situation

The radar technology is known for long time ago, starting with the first experiments of Heinrich Hertz using radio waves in the late 19th century; However, Ground-Penetrating Radar (GPR) is a relatively new technology that was born back in 1910. G. Leimbach and H. Löwy, patented the first equipment to locate buried objects using radar technology. The technique was based on the variations of the conductivity that lead to reflections describing the buried objects. This system, operated with continuous electromagnetic waves, but in 1926, Dr. Hülsenbeck patented a different technology using pulsed radar waves. He noticed that any dielectric variation would produce reflections in the medium (not only conductivity, like the studies of 1910 suggested), and also that this method improved the resolution of the data acquired. Before the GPR studies of 1910 and 1926, the main technique to inspect the soil and the undersurface mediums was Reflection Seismology. Dr. Hülsenbeck observed that his technique had several advantages over Reflection Seismology. (https://www.obonic.de/en/history-ground-penetrating-radar-technology/, consulted on October 2016).

The following years, from the 1930s to the 1970s, approximately, the development of GPR technology grew bit by bit. There were important surveys, like the measurement of the depth of a glacier in Australia in 1927, and other ones like measuring ice depth, probing salt deposits, rock formations in the deserts, inter alia. In that moment, the development for radar systems was more focused on radio communication and moving-targets detection for military purposes in WWII and the Cold War, mainly.

Following the Digital Revolution, between the 60s and the 70s, more computers were affordable and data processing, analysis and storage was easier, so the GPR technology gained general interest. Since then, GPR has been growing fast. In 1985, the first Ground-Penetrating Radar was sold to the general public.

More and more applications have been discovered and lots still to be discovered, yet. Archeology, criminology, structural non-destructive testing, voids detection, agricultural industry soil inspection, pipes detection, etc. GPR still growing and will become a very important technology for non-destructive analysis in the future.

2. Theoretical Bases

The bases for this technology are set in the electromagnetic theories and equations developed by Maxwell in mid-19th Century, who reunite and developed the theories of magnetic and electric fields, which were studied separately before. His theory describes the behavior of electromagnetic fields where variations of charge distributions occur. The first approach to unite electric and magnetic fields with mathematical expressions, was back in 1820, when Hans Christian Ørsted demonstrated that the electric flow through a wire, shook the pointer of a magnetic compass. After that, Faraday and Maxwell studied in detail the relationship of these two fields, resulting into the classical branch of electromagnetism that we know today. Just before them, electric and magnetic fields were studied independently by scientists like Coulomb, Gauss, Biot and Savart, Ampère and Faraday.

After Maxwell established the bases of electromagnetic events, other authors like Lorentz, Oliver Heaviside or Hertz, had contributed to the development and application of Maxwell's equations.

Maxwell's equations and definitions

In the following table you will find Maxwell's equations described and explained:

$\Phi_E = \oint_S \vec{E} \cdot d\vec{S}$	**Gauss's law for electric fields.** The net electric flux (Φ_E) through any closed surface is proportional to the charge inside.
$\oint_S \vec{B} \cdot d\vec{S} = 0$	**Gauss's law for magnetic fields**. The total magnetic flux through a closed surface is zero.
$\oint \vec{E} \cdot d\vec{l} = -\frac{d\Phi_B}{dt}$	**Maxwell-Faraday law of induction.** The voltage induced in a closed circuit ($\oint \vec{E} \cdot d\vec{l}$) is proportional to the rate of change of the magnetic field it encloses.
$\oint_C \vec{B} \cdot d\vec{l} = \mu_0 \int_S \vec{J} \cdot d\vec{S} + \mu_0 \varepsilon_0 \frac{d}{dt} \int_S \vec{E} \cdot d\vec{S}$	**Maxwell extension of Ampère's law.** The magnetic field around a closed loop is proportional to the electric current ($\mu_0 \int_S \vec{J} \cdot d\vec{S}$) plus the displacement current, or rate of change of the electric field ($\mu_0 \varepsilon_0 \frac{d}{dt} \int_S \vec{E} \cdot d\vec{S}$) it encloses.

Fig. 2.1. Maxwell's Equations for electromagnetic fields

Where:

$\vec{E}$ is the electric field vector

$\vec{B}$ is the magnetic field vector

$\vec{J}$ is the current density vector

$\vec{S}$ is the vector area

Φ_E is the electric flux through a certain area.

Φ_B is the magnetic flux through a certain area

$-\frac{d\Phi_B}{dt}$ represents the electromotive force E_{emf}

μ_0 is the vacuum permeability ($\mu_0 = 4\pi \cdot 10^{-7}$ H/m)

ε_0 is the vacuum permittivity ($\varepsilon_0 = 8.854 \cdot 10^{-12}$ F/m)

Maxwell's equations, describe the nature of electromagnetic (EM) waves and its behavior. EM waves, are composed by an electric field (E, measured in [N/C], or [V/m]) and a magnetic field (B, measured in [T], teslas), moving in the same direction and perpendicular between both. As you can observe in the image below, the electric field vector ($\vec{E}$) is perpendicular to *xz* plane, the magnetic field vector ($\vec{B}$) is perpendicular to *xy* plane and $\vec{S}$ is the Poynting vector, perpendicular to *yz* plane that represents the directional energy flux per unit area of both waves. $\vec{S}$ vector is defined as:

$$\vec{S} = \vec{E} \times \vec{H} \qquad [W/m^2] \qquad \textbf{(Eq. 2.1)}$$

Where H is the magnetic field strength defined as:

$$H = \frac{B}{\mu_0} - M \qquad [A/m] \qquad \textbf{(Eq. 2.2)}$$

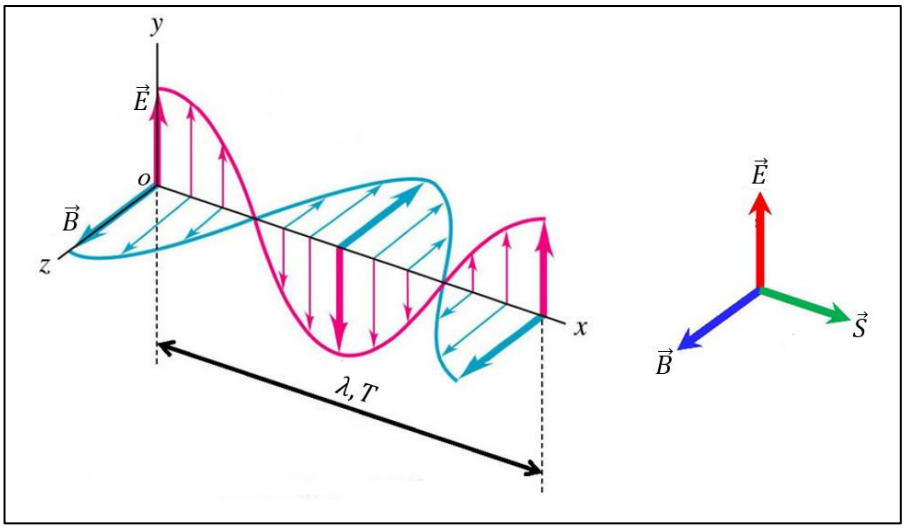

Fig. 2.2. Three dimensional representation of an electromagnetic wave

Being μ_0 the magnetic permeability in the vacuum $\mu_0 = 4\pi \cdot 10^{-7}\ H/m$, and M the magnetization density it has a value of $M = 0$ in the vacuum. Notice that the magnetic field strength H, and the magnetic field B, are only proportional between each other in the vacuum (free space), when $M = 0$. For any other material where an electromagnetic waves travels in, the magnetization density takes more relevance, especially in a magnetizable medium. However, it is safe to approximate $H = B/\mu$ for paramagnetic (e.g. air, aluminum, magnesium…) and diamagnetic (e.g. water, silicon, silver, graphite….) materials. Where μ is the magnetic permeability constant of a material. We will discuss that later.

Other important parameters to define are the wavelength λ, the period T, the frequency f, and the phase velocity v. The period is the time, in seconds, that takes a continuous (sinusoidal) wave to complete one cycle, and the frequency is related to the period by the following expression:

$$f = \frac{1}{T} \qquad [Hz] \qquad \textbf{(Eq. 2.3)}$$

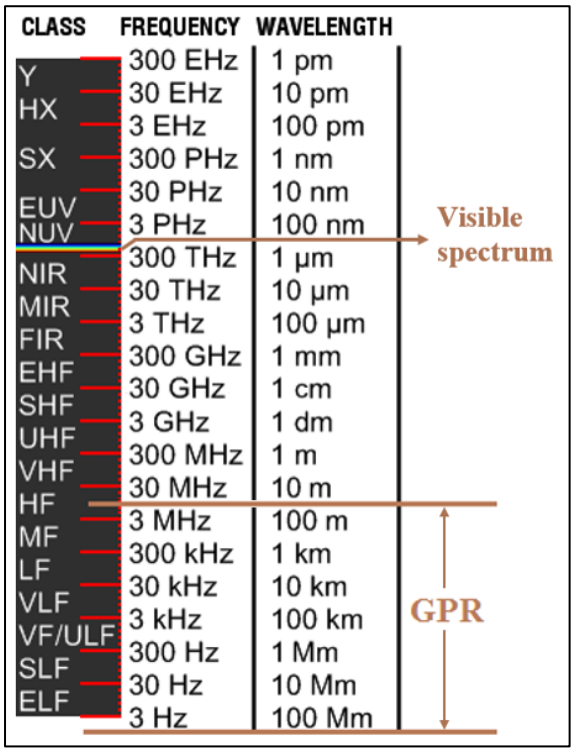

Fig. 2.3. EM waves spectrum breakdown

This two values are related to the wavelength λ through the phase velocity, satisfying the following identity:

$$\lambda = \frac{v}{f} \qquad [m] \qquad \textbf{(Eq. 2.4)}$$

By definition, then, the wavelength is the distance that takes a wave to complete one cycle and the phase velocity is the rate at which the wave propagates in space.

In the vacuum, the phase velocity is defined as $c = 2.998 \cdot 10^8$ m/s. Electromagnetic waves are classified by their frequency or wavelength, taking c as a constant value. For GPR applications, the transmitting antennas are emitting frequencies between 10 MHz and 10 GHz approximately.

Electromagnetic properties of the medium

In the nature, the way how electricity flows, is by free electrons or ions, which create free charges, which are responsible of the conduction of electromagnetic energy. GPR is an efficient technology only in materials with relatively low free charges, because that allows the EM wave to travel within the medium without losing energy in the conduction process. A material containing high level of free charges, is a conductor and the most of the EM energy is lost by heat when a wave hit it. In the field, the majority of surveys are carried out on very heterogeneous materials, where the composition of the soil changes in the 3D space and small-scale heterogeneities appear. This fact makes really difficult to fully understand and represent the electromagnetic properties of each survey, but nevertheless, is very important to study the general properties to loosely understand, the implications of different soil compositions (e.g. water appearance in a wet day, changes in average composition). With that being said, the 3 electric properties mentioned are: conductivity, permittivity and permeability.

2.1.1. Conductivity – σ

As mentioned before, the flow of free electric charges into a material is the reason for conduction currents through it. Conductivity, describes the ability of a material, which is under the influence of an applied field, to pass free electric charges. It is represented by σ, and its units are the S/m, according to the SI.

The equation that describes this property is the following:

$$\sigma = \sigma' - i\sigma'' \qquad \textbf{(Eq. 2.5)}$$

As you can see, the conductivity is composed by a real and an imaginary part. The imaginary part represents the out-of-phase conduction current component of the external current applied, and is usually added to the energy storage effect of the permittivity (we will see it in the next chapter). This imaginary part is more important as the frequency is higher, when part of the physical conduction current of the material and the electric field applied are out of phase (the physical response is lagged in relation to the input current). For GPR applications, where frequencies aren't that high, this imaginary part is negligible, as the lag that is created can be presumed as 0. Then, the conductivity can be represented by its real component, representing the conduction current in phase with the electric field. That way, we can define the conductivity as:

$$\sigma = \frac{J}{E} \qquad \textbf{(Eq. 2.6)}$$

Being J the current density expressed in $[A/m^2\ ]$, and E the electric field, in $[N/C]$. That is, the conductivity is the relation between the current density in the material, and the electric field applied.

The majority of the materials are classified in conductors, semiconductors and insulators depending on their conductivity values in standard condition. In general terms, a conductor will have a conductivity $\sigma > 10^5\ [S/m]$, semiconductors will have a value between 10^5 and $10^{-8}\ [S/m]$ and insulators will be under $10^{-8}\ [S/m]$ for σ.

In addition, this value is highly dependent on the temperature, the composition of the materials, the porosity, and other values such as water saturation or diluted ions' nature. Just as an example, the same soil in the dry season and in the rainy season will present different conductivity; and even more, in the rainy season, the soil may present different conductivity due to the anions and cations (Na^+, Ca^{2+}, Cl^-) that may be diluted in water.

2.1.2. Permittivity – ε

The permittivity describes the ability of a material to store and release EM energy in the form of electric charge. It can also be described as the ability to restrict the flow of free charges or the degree of polarization (in F/m) exhibited by a material under the influence of an applied electric field. It is usually quoted in terms of a nondimensional value (Ground Penetrating Radar Theory and Applications, 2008; chapter 2), it's represented by ε, and its units are the F/m, according to the SI.

The equation for permittivity is as follows:

$$\varepsilon = \varepsilon' - i\varepsilon'' \qquad \textbf{(Eq. 2.7)}$$

Same as conductivity, permittivity is a complex number with real and imaginary part. When an electric field is applied to a material, each pulse induces polarization on the atoms. This polarization switches back and forth as the continuous sinusoidal wave of the electric field goes through the material. This movement of the polarized charges in phase with the electric field (in real life is slightly lagged) creates what we call the storage of energy in the material, and it's represented by the real component ε'. Having this free charges moving in the same rhythm as the electric field applied, produces heat, what is directly translated into energy loss, represented by the imaginary component ε''. The imaginary

term, representing the energy dissipation of the input electric field into heat, takes more importance in this case than the complex part of the conductivity. This component is combined to the imaginary component of the conductivity to get a total loss for the material.

However, it is sometimes simplified to its low-frequency real component, taking as negligible the energy loss represented by the imaginary component in order to get a faster but more general approach to a certain issue. Permittivity can be simplified as:

$$\varepsilon = \frac{D}{E} \qquad \textbf{(Eq. 2.8)}$$

Being D the electric displacement field [C/m^2], and E the electric field. The expression above, is valid for a (ideal) uniform, homogenous, loss-free solid, and can be an approximation for DC currents or low frequency fields.

The permittivity value of a certain material is widely expressed as the relative permittivity ε_r. A nondimensional value that helps with operations, comparisons and mathematical expressions in general. The identity is as follows:

$$\varepsilon_r = \frac{\varepsilon}{\varepsilon_0} \qquad \textbf{(Eq. 2.9)}$$

Relative Permittivity is the Permittivity value of a certain material $\varepsilon = D/E$ in contrast with the permittivity of the vacuum ε_0, which has a value of $\varepsilon_0 = 8.854 \cdot 10^{-12}\ F/m$.

In the table below the influence of frequency in permittivity components for pure water is represented. As you can observe, for low frequencies, the influence of imaginary permittivity is negligible and the real part stays stable. When the frequency starts raising, the increasing amount or energy is transferred to the water that means that the molecules start to polarize faster, which introduces a delay in the response of the water molecules that can't "follow" the frequency of the electric field applied. This leads to more energy loss and the imaginary terms starts raising, while the real component starts to fall. Until the Relaxation frequency, a certain frequency where ε'' has a value as high as it can gets because for higher frequencies, the molecules just can't polarize as fast as the frequency goes so the contrary effect appears: the frequency is so high that some of the polarization just don't happen, and gradually more and more molecules get back to 0-polarization state. That's why both real and imaginary component falls.

This effect of dielectric heating can be seen in microwaves oven, which work with frequencies around 2.5 GHz.

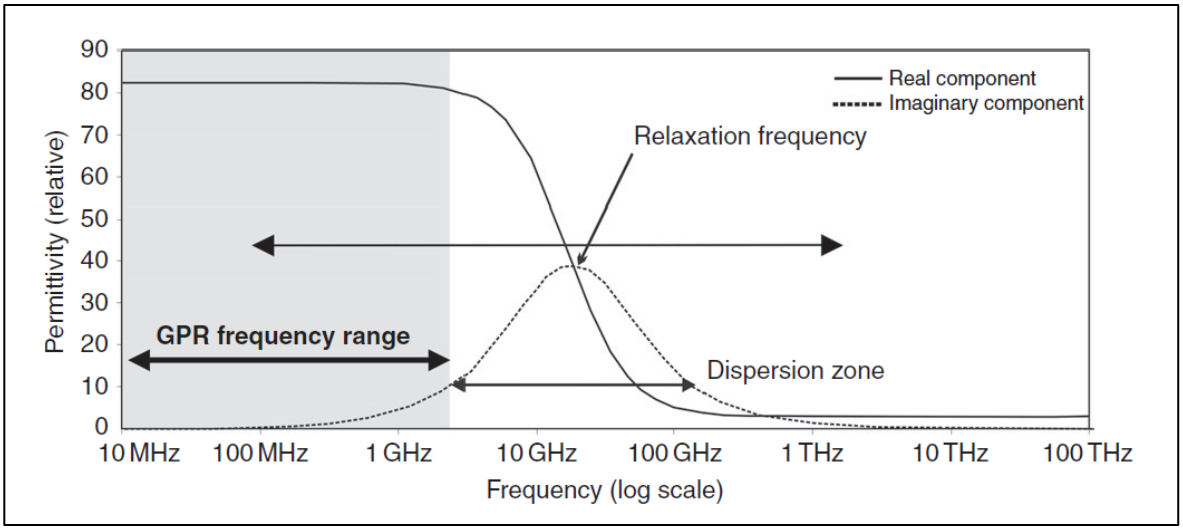

Fig. 2.4. Relative permittivity real and imaginary components against frequency. *Ground Penetrating Radar Theory and Applications, 2008*.

However, this table is only valid for pure water. Solid materials experiment different polarization states and water presence in the soil affects in the permittivity (real and imaginary), being possible to create different tables for different materials and water content on each one. For example, in some solid materials with very few water content, the curves in the table before move over the low frequency range. For other materials, the imaginary permittivity has more than one peak in the Relaxation Frequency, this is utilized in Diathermy, a medicine process to heat up local tissues.

2.1.3. Permeability – μ

It defines the degree of magnetization of a material. That is, in other words, the capacity of a certain material to form a magnetic field within itself when is influenced by an external magnetic field. The property has units of $[H/m]$, according to the SI and is denoted by the Greek letter μ. The permeability of the vacuum is a commonly used constant known as the magnetic constant μ_0, with a value of $\mu_0 = 4\pi \cdot 10^{-7} H/m \approx 1.2566 \cdot 10^{-6} H/m$. Same as the conductivity and the permittivity, permeability is a complex number with the real part representing the static behavior of the material against an external field and the imaginary part represent the energy loss.

For GPR applications, the permeability is commonly neglected because of the composition of the majority of the soils surveyed. On Earth, the majority of the components in the ground are diamagnetic or paramagnetic, where the magnetization effect does not affect the GPR waves in a significant way.

In these cases, the permeability is approximated to the permeability of the vacuum μ_0; and therefore, the relative permeability $\mu_r = \frac{\mu}{\mu_0} = 1$.

However, not all the materials in the ground are magnetic-insignificant materials. We can easily find iron rich terrains, metallic oxides and other ferromagnetic minerals and despite these materials are not the most common on Earth, they can affect the velocity and attenuation of the waves.

Electromagnetic properties of the wave

Electromagnetic wave's properties are material-dependent and electromagnetic material properties are frequency dependent (permittivity changes, when changing the frequency, for example), so, the properties of a wave will be material and frequency dependent, as we will see in the following topics. For the most GPR surveys, we will be working with materials that can be supposed as perfect dielectrics ($\mu_r = 1;\ \sigma < 10^{-8}$). In the graphics below, you can observe how velocity and attenuation changes depending on the frequency.

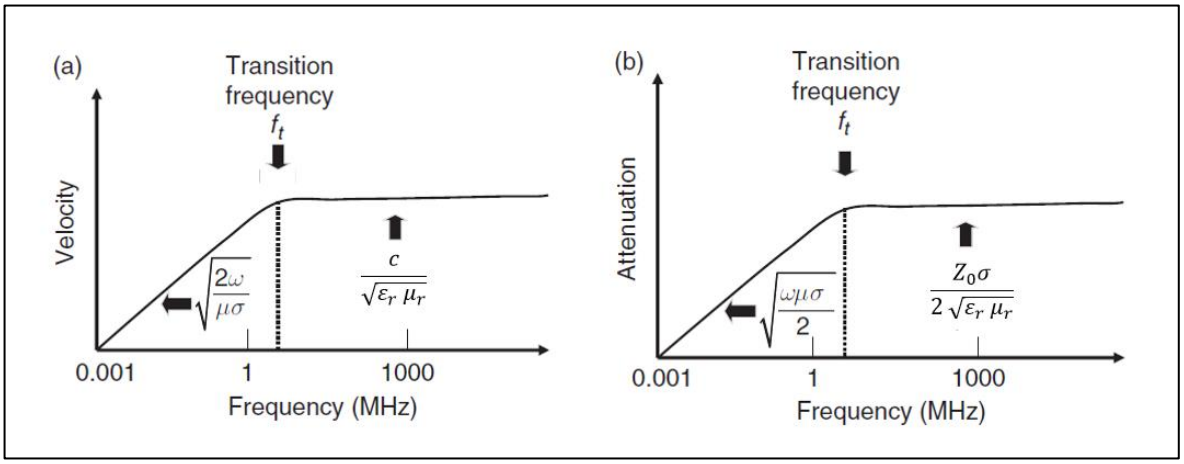

Fig. 2.5. Velocity and Attenuation behavior depending on. *Ground Penetrating Radar Theory and Applications, 2008*.

Surprisingly as it is, for frequencies above the Transition Frequency (f_t), the electromagnetic properties of the waves, behave almost constant.

$$f_t = \frac{\sigma}{2\pi\varepsilon} \qquad \textbf{(Eq. 2.10)}$$

This constant value is useful for GPR applications, as the majority of the antenna's frequency are between 10MHz to 10GHz, ensuring that way the constant behavior of the EM in GPR.

2.1.4. Velocity – v

Solving Maxwell differential equations with certain boundary conditions, we can obtain a term that contains information about the velocity and the attenuation of the electromagnetic waves. This terms is known as the propagation constant γ:

$$\gamma = \alpha + i\beta \quad \textbf{(Eq. 2.11)}$$

Where α is the real part, also known as the attenuation constant (see next section); β is the imaginary part and it is called phase constant. The term γ is a non-dimensional constant and represents the amplitude and phase changes of a wave as it propagates in a known direction.

The expression that gives us information about the velocity, is the imaginary phase constant β, defined as follows:

$$\beta = \frac{\omega}{v} = \frac{\omega}{c} Re\sqrt{\varepsilon_r \mu_r} \quad \textbf{(Eq. 2.12)}$$

Where v is the phase velocity of the electromagnetic wave:

$$v = \frac{c}{Re\sqrt{\varepsilon_r \mu_r}} \quad \textbf{(Eq. 2.13)}$$

Being c the velocity of an electromagnetic wave in free space ($c = \frac{1}{\sqrt{\mu_0 \varepsilon_0}} = 2.998 \cdot 10^8$ m/s), $\varepsilon_r \; and \; \mu_r$ are the relative permittivity and permeability of the medium respectively.

If we take into consideration that for non-magnetic materials $\mu_r \approx 1$, and also that for GPR applications the imaginary part of the permittivity can be considered negligible in front of the real part (as seen in permittivity section), we can rewrite the expression above as:

$$v = \frac{c}{\sqrt{\mu_r \; \varepsilon_r}} \cong \frac{c}{\sqrt{\varepsilon_r}} \quad \textbf{(Eq. 2.14)}$$

The fastest medium on Earth where an electromagnetic wave can travel through (excluding vacuum) is air, with a value of 0.3 m/ns. On the other hand, water is the medium where EM waves had the

slower phase velocity: around 0.034 m/ns. For ground materials, typical velocity values go around 0.5 m/ns to 0.15 m/ns depending in most cases of porosity (where the velocity would be faster) and water content (where velocity would be slower).

2.1.5. Attenuation – α

As discussed before, the propagation constant γ gathers the information about the velocity and attenuation of and EM wave. Attenuation in this case, is the real part of the propagation constant and similarly to the phase constant, attenuation constant is defined as:

$$\alpha = \frac{\omega}{c} Im\sqrt{\varepsilon_r \, \mu_r} \qquad \textbf{(Eq. 2.15)}$$

This concept represents the decrease of the amplitude of a given EM wave while it travels through medium from the start point. However, this expression can be simplified as:

$$\alpha = \frac{1}{2}\sigma\sqrt{\frac{\mu}{\varepsilon}} = Z_0 \, \frac{\sigma}{2\sqrt{\varepsilon_r \, \mu_r}} \qquad \textbf{(Eq. 2.16)}$$

Where Z_0 is the electromagnetic impedance of free space in Ohms ($Z_0 = \sqrt{\varepsilon_0/\mu_0}$). The equation above only works with non-magnetic materials in case of the frequencies used in GPR, nevertheless, the attenuation has a frequency dependency that needs to be discussed. Water content in mediums absorbs more and more energy as the frequency increase and thus, the attenuation also increases. Common values for the attenuation constant are around 1 dB/m.

2.1.6. Electromagnetic impedance – Z

Electromagnetic impedance or wave impedance, is defined as the relation between the electric and the magnetic field, perpendicular between each other:

$$Z = \frac{\vec{E}}{\vec{B}} \qquad [\Omega] \qquad \textbf{(Eq. 2.17)}$$

Is interesting to point, that for non-magnetic materials, electromagnetic wave impedance and material impedance are the same, and we can define electromagnetic impedance of a wave by the EM material properties. Then, it can also be defined:

$$Z = \sqrt{\frac{i\omega\mu}{\sigma + i\omega\varepsilon}} \qquad [\Omega] \qquad \textbf{(Eq. 2.18)}$$

Where i is the imaginary unit and ω is the angular frequency of the wave ($\omega = 2\pi f$). Following the same principles that we applied before, we can simplify this equation and adapt it to GPR surveys (frequencies between 1Hz and 5GHz), becoming:

$$Z = \sqrt{\frac{\mu}{\varepsilon}} \qquad [\Omega] \qquad \textbf{(Eq. 2.19)}$$

That way, the impedance of free space is $Z_0 = \sqrt{\frac{\mu_0}{\varepsilon_0}} = 120\pi\ \Omega$. We can also define the impedance of a dielectric referred to the impedance of free space, taking into consideration that $\mu = \mu_0 = 4\pi \cdot 10^{-7}\ \mathrm{H/m}$:

$$Z = \sqrt{\frac{\mu}{\varepsilon}} = \sqrt{\frac{\mu_0}{\varepsilon_0 \varepsilon_r}} = \frac{Z_0}{\sqrt{\varepsilon_r}} \approx \frac{377}{\sqrt{\varepsilon_r}} \qquad [\Omega] \qquad \textbf{(Eq. 2.20)}$$

Some typical impedance values for ground materials are between 100-150 Ω.

Reflection, refraction and transmission

When an electromagnetic wave travelling through a certain medium (with homogenous properties), encounters the surface of a different medium with different electromagnetic properties, the energy of the incident EM wave is split in two different waves: the reflected and the refracted wave. The simplest model to explain this phenomenon is composed by an EM wave travelling through the medium 1, which is in contact with medium 2 by a flat horizontal surface interlayer. When the wave encounters the medium 1 with an incidence angle of θ_i, on one hand is reflected with a reflection angle θ_r, satisfying $\theta_i = \theta_r$. On the other hand, the wave is refracted and transmitted to medium 2 with and angle θ_R. This explanation is based on the law known as the Snell's law, named after Willebrord Snellius (1580-1626). The law states the following:

$$\frac{sin\,\theta_1}{\sin\theta_2} = \frac{v_1}{v_2} \qquad \textbf{(Eq. 2.21)}$$

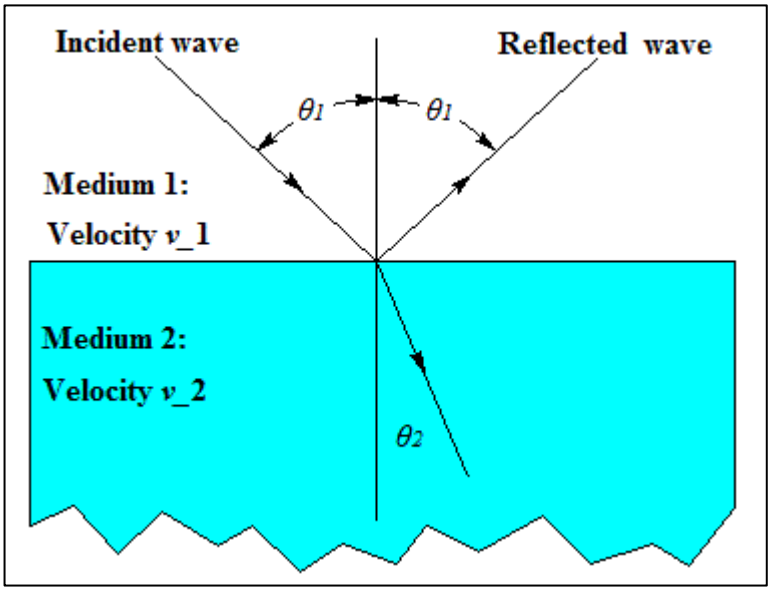

Fig. 2.6. Snell's law representation

As you can observe in the image, if the velocity doesn't change, the reflected angle is the same as the incident angle in relation to a perpendicular line to the interlayer surface in the incidence point.

On the other hand, we need to consider the energy transmission of the electromagnetic field. In order to break that down, we need to stick to the law of conservation of energy. According to the example above, the transmission coefficient (T) represents the part of the energy that goes through the medium 2 and the reflection coefficient (R) represents the part of the energy that travels to the medium 1. The value of T and R and thus, the quantity of energy that is either reflected or refracted depends on the intrinsic impedance (Z) of the materials. This was stated by Fresnel:

$$R = \frac{Z_2\,cos(\theta_2) - Z_1\,cos(\theta_1)}{Z_1\cos(\theta_1) + Z_2\,cos(\theta_2)} \qquad \textbf{(Eq. 2.22)}$$

$$T = \frac{2Z_2 cos\theta_2}{Z_1\,cos(\theta_1) + Z_2\,cos(\theta_2)} \qquad \textbf{(Eq. 2.23)}$$

$$1 = T + R \qquad \textbf{(Eq. 2.24)}$$

Where θ_i is the angle with respect to the perpendicular line to the interface in the incidence point. As you can observe, the subscript 1 or 2, on the equations are referring to the medium 1 or 2 respectively. Notice that, θ_1 is referring to both the incidence and the reflection angle, as the Snell's law states and θ_2 represents the refraction angle.

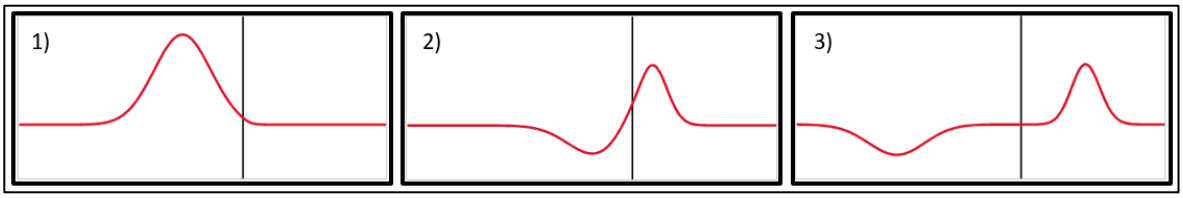

Fig. 2.7. Single wave amplitude representation of reflection. 1) Wave is going through medium 1. 2) Wave is trespassing the limit of the two mediums and reflection has begun. 3) Both reflected and transmitted waves can be after the reflection.

The reflection and transition phenomena can also be descried according to energy conservation if we take into consideration the amplitude of the wave. This is, the reflection coefficient represents the energy reflected in front of the input energy and the transmission coefficient represents the energy refracted in front of the input energy, thus we can write:

$$r = \frac{A_r}{A_i} \qquad \textbf{(Eq. 2.25)}$$

$$t = \frac{A_t}{A_i} \qquad \textbf{(Eq. 2.26)}$$

Being A, the amplitude of the wave and the subscripts standing r for reflected, i for incidence or input and t for transmitted. Both coefficients –the ones obtained from the angles and the ones obtained from the amplitudes-, are related between each other with the following identity:

$$R = r^2 \qquad \textbf{(Eq. 2.27)}$$

$$T = t^2 \qquad \textbf{(Eq. 2.28)}$$

Resolution

When doing a GPR survey, there are two aspects that we need to keep in mind to have a proper GPR study. Those are the Vertical and Horizontal resolution. From the information that we get from its names, we can deduce that the Horizontal Resolution allows us to predict, if two different targets located near to each other and in the same horizontal plane (depth), will be recognizable in the radargrams, as two different reflections or just one. In the other hand, the Vertical resolution, allow us to differentiate two different return pulses of the wave as two different targets when they are located in the same direction in which the antenna wave travels.

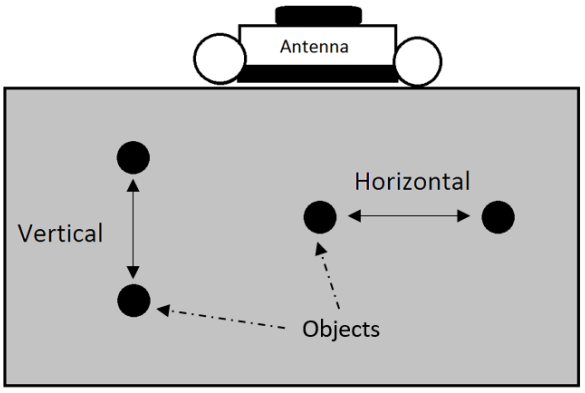

Fig. 2.8. Vertical resolution is related to reflectors at different depth and horizontal resolution to reflectors at same depth.

2.1.7. Horizontal Resolution

Getting into more detail, the horizontal resolution, depends on four factors:

- The number of traces obtained (traces/s or traces/m)
- The shape of the beam
- The footprint of the antenna
- The depth of the target.

A trace is a record of the reflection of the electromagnetic wave sent into the surveyed material. A lot of traces disposed one next to each other is how radargrams are created. That way, the number of traces is the number of records that you want to obtain in a certain distance or in a certain time. This is an adjustable value that is typically set before the survey starts. Usually, the more traces the antenna can get, the better the resolution will be.

The primary EM waves that the antenna is sending to the surveyed zone, shape a primary lobe, which usually is geometrically approximated to a cone (the base of the cone is not always a circumference, and depending on the manufacturer, it may be an ellipse). This cone, intersects the target, to receive back the energy that it reflects. The shape of this lobe (or cone) depends on the system manufacturer and the electromagnetic properties of the material. The narrower the lobe is, the better the horizontal resolution will be.

Regarding the footprint of the antenna, we can refer to it like the area that the beam is able to reflect on. Similar when a flashlight is pointed to a wall, we can see an area that the flashlight is illuminating and out of that zone, the wall is dark. The wider the footprint, the worst the H. resolution will be, because it won't detect smaller areas than the footprint. There are different ways to calculate this footprint area.

The footprint area can be approximated to the area left by the 1st Fresnel zone. Before the equation, a little explanation is important:

When an EM wave is sent from the transmitter, it is spread in all directions, but the most of the energy takes the direction where the transmitter is pointing at. Taking into consideration that the wave that has a perpendicular direction to the transmitter is the fastest one, the other waves will be "slower", thereby, with a different phase. The first Fresnel zone is the limit where inside this zone, the phase difference is under 180º; and out of this zone the phase difference is over 180º. For more information about the 1st Fresnel zone in GPR, you can check: "Pérez Gracia, Vega. 2001. *Radar de subsuelo. Evaluación para aplicaciones en arqueología y en patrimonio histórico-artístico*". Thus, one way to calculate the footprint area is:

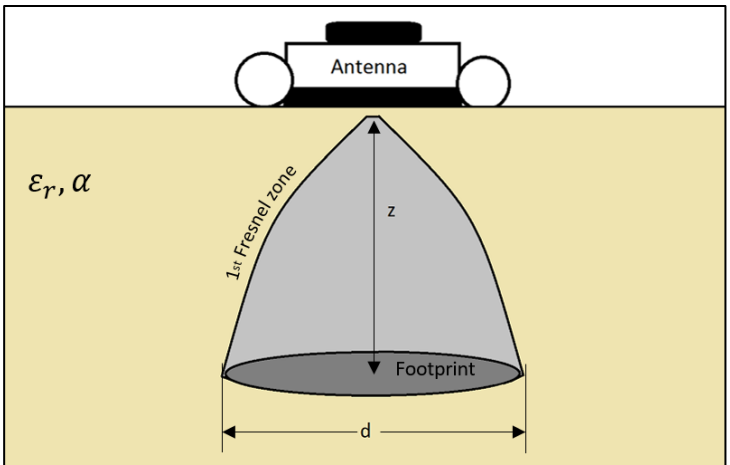

Fig. 2.9. Footprint plays a huge role on understanding horizontal resolution.

$$d = \sqrt{\frac{\lambda^2}{4} + z\lambda} \qquad \textbf{(Eq. 2.29)}$$

Where z is depth, λ is the wavelength and d is the diameter of the footprint.

Other authors, state that we can calculate the footprint using the attenuation coefficient α of the medium. This coefficient, is a widely used concept in wave or beam propagation studies, and determines how easily a medium can be penetrated by a beam, taking into consideration the electromagnetic properties of the medium like the permittivity, ε or the permeability, μ. We can notice that for the same depth, a high attenuating medium, will have a narrower footprint, in other words, a better resolution.

$$d = 4z\sqrt{\frac{ln2}{(2+\alpha z)}} \qquad \textbf{(Eq. 2.30)}$$

Another equation to calculate the footprint diameter, (Rial, Fernando I.; Pereira, Manuel; Lorenzo, Henrique; Arias, Pedro and Novo, Alexandre. 2007) emphasizes the wavelength and the permittivity of the medium. For the majority of the GPR surveys in archeology and civil engineering, the electric permittivity is more relevant than the magnetic permeability, because we will rarely find a magnetizable soil or structure. It defines the horizontal resolution as:

$$r = \frac{\lambda}{4} + \frac{z}{\sqrt{\varepsilon_r + 1}} \qquad d = 2r \qquad \textbf{(Eq. 2.31)}$$

Where ε_r is the relative permittivity.

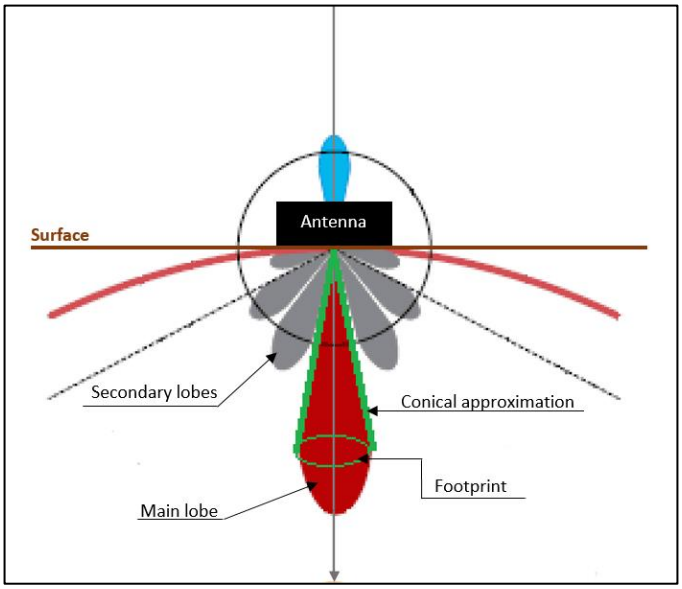

Fig. 2.10. Wave propagation can be represented by lobules coming from the antenna and propagating to all directions

The depth of the reflector, also affects to the resolution: too close to the antenna, and it will be affected by equipment noise due to the interaction between the transmitter and the receiver; too far from the antenna, and the waves will have been so attenuated that the target won't be recognizable. This information is reflected in all the equations described before.

In addition, there are different experimental-based values which provide us information about it as well. (Conyers, Lawrence B., 2016).

2.1.8. Vertical resolution

The capacity of the equipment to discriminate the return pulses of two consecutive targets as one reflection or two different ones is the vertical resolution. It is dependent on the bandwidth (Δf) and the duration of the radar pulse (ΔT), that are inversely proportional between each other.

$$\Delta T = \frac{1}{\Delta f} \qquad \textbf{(Eq. 2.32)}$$

Below, some examples of the duration of the pulse depending on the bandwidth of the antenna.

Bandwidth Δf	Duration of the pulse ΔT
2.3 GHz	0.435 ns
1.6 GHz	0.625 ns
1.2 GHz	0.83 ns
1 GHz	1 ns
900 MHz	1.1 ns

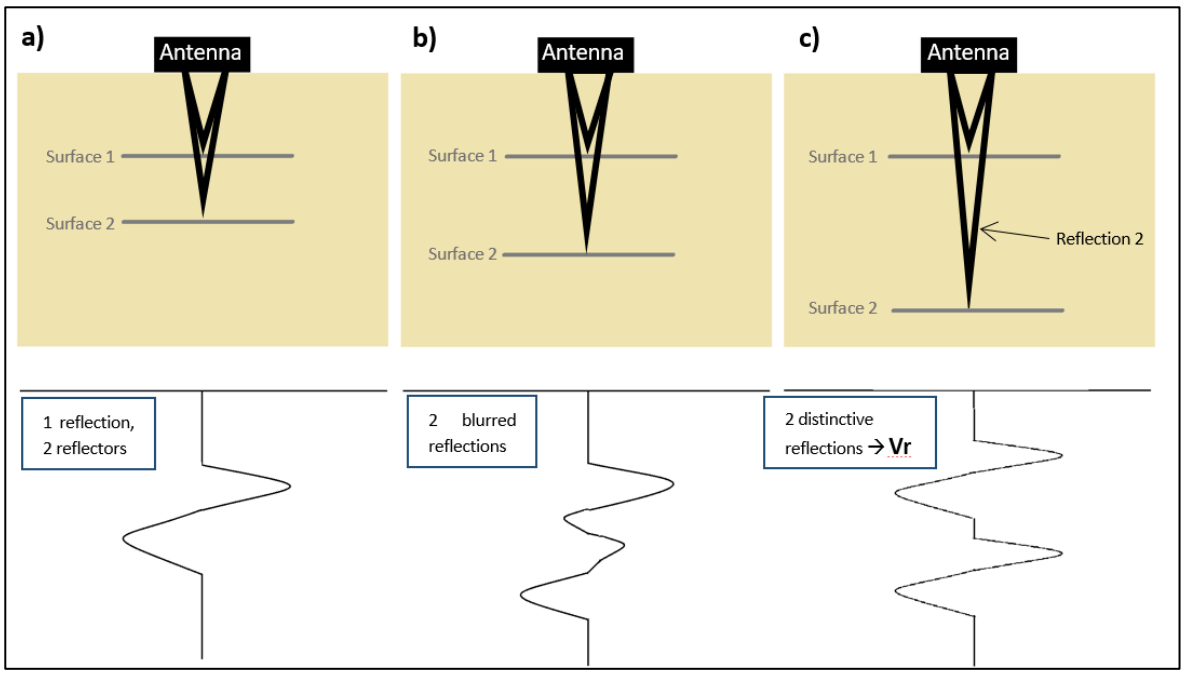

Fig. 2.11. Scheme on how vertical resolution behaves

Each EM pulse, is separated form the next by a certain distance depending on the velocity propagation of the wave in the medium. This distance allows us to set a numerical value to the Vertical resolution (Vr from now on). Beforehand, we could state that higher frequency antennas will have better Vr. Even though this statement is right, it is not 100% true. In this case, dielectric and physical characteristics of the propagation medium are very relevant because they will change the velocity of the electromagnetic waves. To define a Vr number we need to take into consideration that: setting two consecutive surfaces (in the direction of the wave), the reflection of the first surface needs to be completely represented in the radargram before the reflection of the second surface appears, for considering the minimum distance for Vr.

Wtih this consideration in mind, and taking the pulse lenght as the product of the duration of the pulse (ΔT) and the velocity of the wave in the medium, we can define the vertical resolution as:

$$Vr = \frac{v}{\Delta f} = \frac{v\Delta t}{2} \qquad \textbf{(Eq. 2.33)}$$

Where v is the velocity of the wave in the medium, and Δt is defined as:

$$\Delta t = 2T = \frac{2}{f} \qquad \textbf{(Eq. 2.34)}$$

As the velocity of an electromagnetic wave is as follows:

$$v = \frac{c}{Re\sqrt{\varepsilon_r \mu_r}} \qquad \textbf{(Eq. 2.35)}$$

Then, the vertical resolution Vr can be rewritten as:

$$Vr = \frac{c}{\Delta f \; Re\sqrt{\varepsilon_r \mu_r}} \qquad \textbf{(Eq. 2.36)}$$

Where ω is the angular velocity (rad/s), c is the velocity of the wave in the vacuum, $\varepsilon_r \; \mu_r$ are the relative permittivity and permeability respectively. We can notice that the bigger the dielectric constants are, the smaller the velocity is (for the same frequency). That means that the Vertical

resolution will be better (will decrease) when the dielectric constants of the medium are bigger, in other words, when the propagation velocity of the wave decreases.

Some authors, even rewrite the equation of the vertical resolution, adding a multiplying factor of 1.39 in order to consider the effects of natural heterogeneous materials. This factor is obtained from empirical experiments and using it ensures that the actual resolution will be equal to the result of the equation or better, no worse (Ground Penetrating Radar Theory and Applications, 2008; chapter 3). Then:

$$Vr = \frac{1.39\ c}{\Delta f\ Re\sqrt{\varepsilon_r \mu_r}} \qquad \textbf{(Eq. 2.37)}$$

This last equation, take in consideration the attenuation effect that the medium applies to EM waves (in the worst scenario). To the EM waves, the soil applies a "low-pass" filter effect that absorbs high frequency components. This effect is caused mainly for the attenuation effect of natural mediums and for the reflection of the wave when leaving the antenna and passing through the surface of the medium.

2.1.9. Range resolution (resolution between radargrams)

In order to make 3D images of the buried objects, we need to understand the 3D match that software works with in order to generate images from radargrams. There are two ways that the software mainly processes data: by interpolation between radargrams and by dense gridding between them. Typically for archaeology surveys is more efficient to use interpolation between radargrams due to the large surveyed areas of terrain, where radargrams are spaced from 0.5 to 5 meters and software uses interpolation between data to generate the 3D volumes. In these studies, a very high resolution is not a must, but is more important to represent with fidelity the targets underground. A good example is a survey to find ancient buildings buried underground where the goal is to understand the disposition of the various buildings and space the radargrams under 0.5 meter won't be efficient because of the time and energy spent on the survey.

When one needs to study smaller targets and high resolution is required to represent small details of the targets, we need to use dense (or ultra-dense) gridding surveys and therefore, the software won't need interpolation between radargrams to generate the 3D volumes. In those cases, the space between the radargrams has to be smaller, typically between 1 to 50 cm (in some cases less than 1 cm).

To help us in this matter, we have the Nyquist-Shannon sampling theorem that stablishes the minimum sample rate, which allow discrete samples to represent a continuous signal without losing information. Given a continuous frequency wave, this theorem specifies the frequency of the samples in order to represent the input wave with fidelity to avoid aliasing.

Aliasing is a very common phenomenon produced when the sampling rate is too low to gather the full information of the input data and leads to wrong representation of the initial information. To understand this aliasing effect, we can see an example of sampling a continuous sinusoidal wave with discrete samples. As you can notice in the image below, the input signal (in blue) is sampled at a certain frequency –represented by the sampling clock, in pink-. At the time to take the samples and represent them trying to match the input signal, the represented wave is completely different –represented in red-.

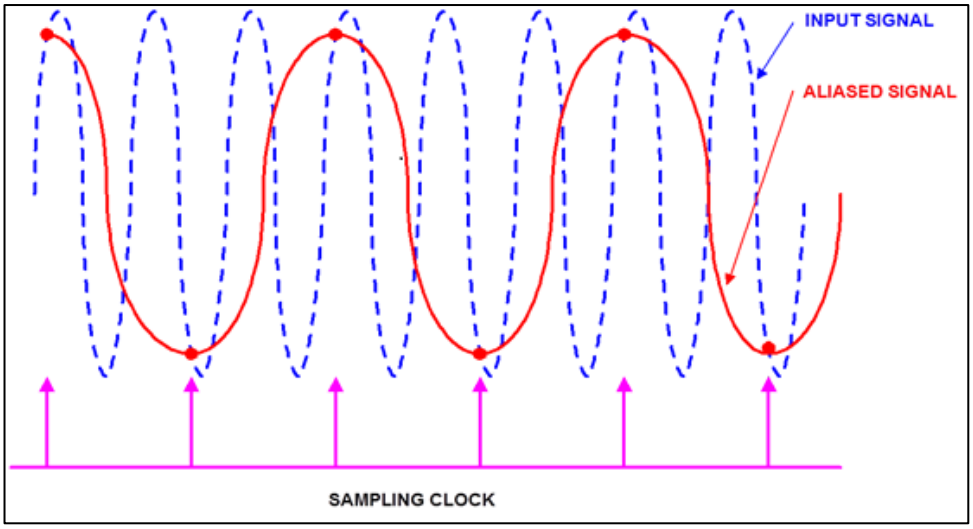

Fig. 2.12. Sampling an input signal at lower frequencies than this signal produces aliasng

Nyquist-Shannon theorem specifies that for a given continuous input signal $x(t)$, with maximum frequency $F_{max} = B$, the minimum sample frequency F_s, must be $F_s > 2F_{max} \equiv 2B$, in order to be able to fully represent the input signal $x(t)$. This theorem is considerably more dense and deep than the explained here, but for the subject of study of this project is adequate to understand this simple concept only.

In the specific case of 3D imaging with GPR radargrams, we are going to use this theorem to define the minimum theoretical distance between radargrams (samples) to avoid aliasing and fully represent with high resolution the underground targets. The relation between the concept explained before and the our GPR survey is, in general terms, is that the targets to study are the continuous sinusoidal wave and the sample rate is the distance between radargrams to generate the 3D volume.

Nyquist-Shannon stablish that the sampling interval is one quarter of the wavelength (Novo, Alexandre; Grasmueck, Mark; Viggiano, Dave A. and Lorenzo, Henrique. 2002) in the host material, expressed as:

$$n_x = \frac{c}{4f\sqrt{\varepsilon_r}} = \frac{75}{f\sqrt{\varepsilon_r}} \qquad \textbf{(Eq. 2.38)}$$

Were:
n_x is the sampling interval (in m)
f is the center frequency of the antenna (in MHz)
ε_r is the relative permittivity constant of the host medium

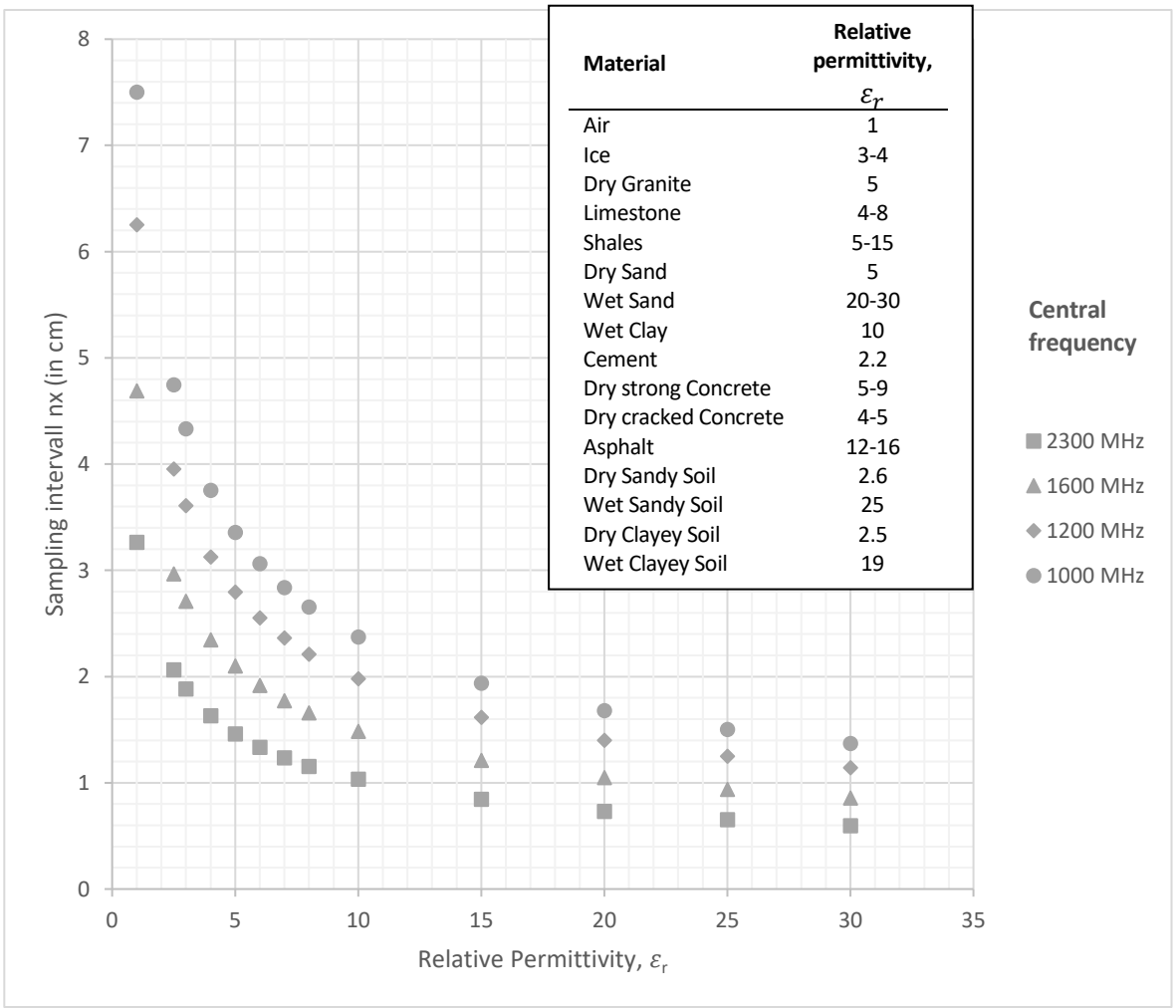

Material	Relative permittivity, ε_r
Air	1
Ice	3-4
Dry Granite	5
Limestone	4-8
Shales	5-15
Dry Sand	5
Wet Sand	20-30
Wet Clay	10
Cement	2.2
Dry strong Concrete	5-9
Dry cracked Concrete	4-5
Asphalt	12-16
Dry Sandy Soil	2.6
Wet Sandy Soil	25
Dry Clayey Soil	2.5
Wet Clayey Soil	19

Fig. 2.13. Sampling interval against relative permittivity for different antennas frequencies, along with a table of relative permittivity of different soils

As you can see, for high frequency antennas, the sample rate distance will be less than 5 cm in the most cases.

Energy loss in EM waves

Inevitably, natural environments are heterogeneous almost by definition and ground penetrating radar signals are affected by this complexity of the mediums that had heterogeneous electromagnetic properties through all directions.

2.1.10. Scattering

Scattering is the definition of the energy loss due to very small electromagnetic changes on the medium that continuously apply reflection and refraction to the EM wave through its path on the soil and spread small parts of the wave in all directions. The losses are undetectable if we study them by separate but all this microscopic heterogeneities summed through all the travel distance of the wave, generate an energy loss that affects the receiving signal.

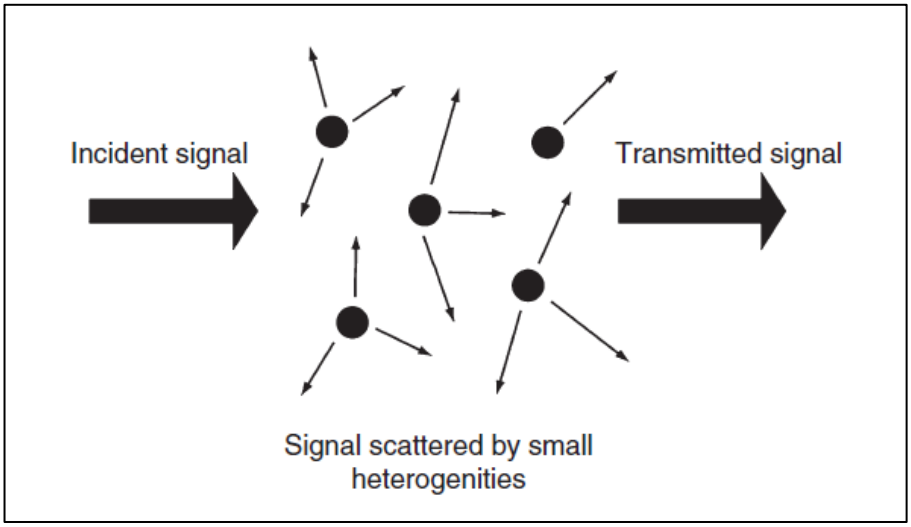

Fig. 2.14. EM waves present scattering when going through small heterogeneities, which reduces output amplitudes. *Ground Penetrating Radar Theory and Applications, 2008*.

This effect is very frequency dependent, as for higher frequencies, the wavelength is shorter and thus, it exists more probability for the signal to hit this small scatters.

Some authors also enclose other effects as scattering, such as the energy losses when the wavelength is greater than the size of the medium where the wave is traveling through. For example in a laboratory test where some kind of artificial medium is prepared and the boundaries of the medium are shorter than the wavelength. This effect will generate a noise on the receiving signal.

3. How GPR works

The ground penetrating radar is a non-invasive technique to evaluate targets inside a travel medium. The main GPR system is typically composed by one or more antennas, a central control unit and a data recording system. The antenna is in charge of emitting and receiving the electromagnetic waves, which are recorded by the recording system and then stored, processed and displayed by the control unit. It is usual to see other accessories attached to the main equipment, such as odometers, coordinate tracking systems (GPS, laser guides), screens, printers or keyboards.

The simplest configuration is composed for one transmitter and one receiver antenna and both are controlled by the control unit. This control unit, send impulses to the transmitter, which through electric fields creates electromagnetic waves that are sent to the medium in which the wave travels without changes since the dielectric properties of the mediums change. When there change in the medium (other material or target) is encountered, part of the energy from the EM wave, is reflected in all directions. Then, the receiver record part of the reflected electromagnetic wave and creates an electric pulse that travels back to the control unit and is recorded. After being recorded, the control unit, processes the signal and creates a digital representation of the pulses received by the receiver. Via software, the digital representation of all the signals received are collated, stored and displayed in what we know as radargrams. Radargrams are the digital representation of all the data gathered by the receiver through a certain survey distance, and allow us to understand what is below the surface.

Radargram

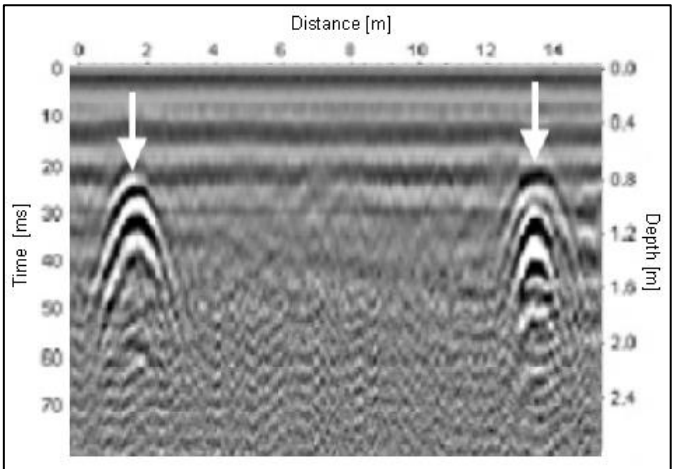

Fig. 3.1. Radargram representation. This is how a radargram looks like with two differentiated reflectors

A radargram is a two-dimensional digital representation of the travel time of the waves since they leave the transmitter until they reach the receiver antenna. The receiver antenna records an analog signal with information about the travel time of the wave and its amplitude (energy). This information is later processed and with the information of various waves the radargram is formed. The travel time (that can be translated to depth if we have the velocity of the wave) and its amplitude is represented in the abscissa axis, the ordinate axis can either represent the time in which the antenna is recording or the distance surveyed for it.

Antenna

The antenna of a GPR system is the part of the equipment that emit or receive the electromagnetic waves. Some devices have more than one antenna, for example, one for emitting and one for receiving or even more than two in order to array the phases and create more complex GPR surveys. For ground penetrating radar, the antenna is composed for separated transmitter and receiver elements, while for other purposes (like aero navigation) the transmitter and the receiver are the same element. Imagine, for example, the antenna of an air traffic control tower; in this case the transmitter and the receiver are the same element, but for GPR uses, the antenna must have different elements for each function (there are some GPR systems with a single antenna, but the majority of them are made with separate transmitter and receiver antennas).

The reason for using separate transmitter and receiver antennas is because of the difficulty on the operation of coordinate and manage EM waves having a single antenna for transmitting and receiving. That means that the antenna would have to switch from transmitter to receiver before the reflection of the initial transmitted beam arrives to the antenna. As you can imagine, the closer the reflector is, the fewer time it takes the reflection to hit the antenna, so the switch needs to be ultra-fast in order to overcome nanosecond magnitude times. Moreover, the switch needs to be done with ultra-high isolation between transmitter and receiver to avoid influencing the measure. This is unfeasible for the most of the GPR surveys and only a few studies with very specific targets, which makes using a single transmitter and receiver antenna worth, actually uses it.

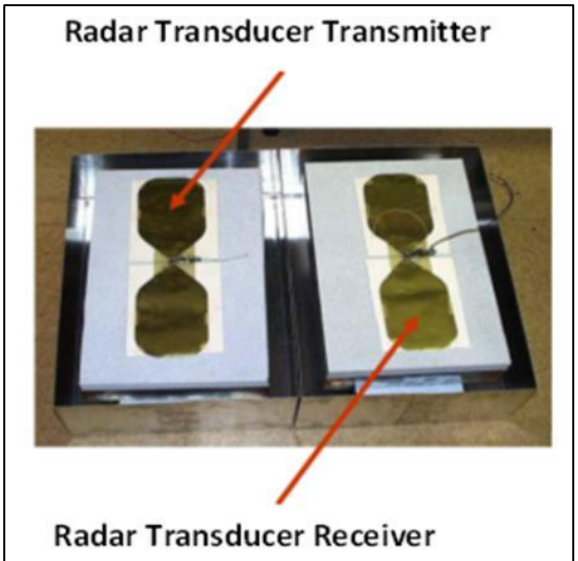

Fig. 3.2. Bow tie antenna from the inside

Through the time there have been various antenna types, the most used nowadays are wired antennas, time domain antennas composed by conductive wires where the current flows by and produces the electromagnetic waves that travel through the material. These wires are mostly manufactured forming loops or helixes with different shapes: rounded, squared, triangular, bow-tied and other shapes.

Control unit

The control unit (CU) is one of the fundamental parts of a GPR system. Its functions are to emit pulses to the transmitter, amplify pulses received by the receiver, process the signals, supply the antenna of power and manage all the different accessories that can be connected such as monitors, keyboards, odometers or printers. Some control units are also capable to storage data, convert analog pulses to digital data, apply filters and modify the signals in the field; however, nowadays this functionalities are done by a PCs or similar systems designed for this purposes. In case of multi-channel surveys, the control unit is the responsible of manage the different signals.

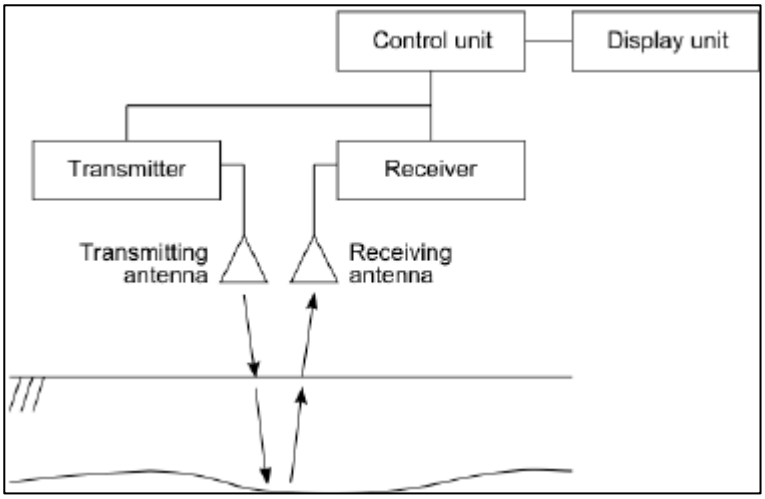

Fig. 3.3. Basic scheme of a GPR control unit and antenna connections

Different types of antennas, require different control units to operate them, so for each survey the appropriate antenna-CU tandem must be chosen. It is a common practice to connect the control unit to a digital monitor, where the signal received by the antenna is shown in real time. In some monitors, one is able to change the signal visualization and even modify the signal (apply gain, dewow, etc.); in others, it only shows the signal as it is recorded by the antenna.

Some GPR manufacturers are even selling products for brief/slight surveys with all the functionalities described before compacted in one device.

4. GPR Equipment and software

In this section, the GPR equipment used for the experimental acquisition of data will be described. As well as the software utilized for the processing and analysis of the data. For the field survey, we will be working with an antenna and control unit form the manufacturer a MALÅ Geoscience. On the other hand, GPR-SLICE version V7.0 is the main software utilized for this project, although we will be also working with ReflexW version 5.5.1 and RAMAC GroundVision version 1.4.1 from MALÅ Geoscience.

For field surveys the MALÅ Geoscience systems is composed by 3 main elements: the multi-channel control unit RAMAC CUII, the 1.6GHz HF shielded antenna, and the monitor RAMAC XV11. Additionally we will also need an 8V Li-Ion battery to power the control unit, a 12V Li-Ion battery for the monitor and a wheel-cart with an odometer attached to the antenna.

4.1.1. RAMAC CUII Control Unit

The control unit CUII is very versatile and it's capable of manage antennas in the range of 25MHz – 2.3GHz, designed for a very large range of surveys from archeology purposes to civil engineering surveys. This particular model allow us to connect an external module to have multi-channel performance and have 4 or 16 channels. However, we will use a single channel functionality for this work. The 8V battery gives us a full autonomy of around 3 hours. In the following table, the specifications of the device are described.

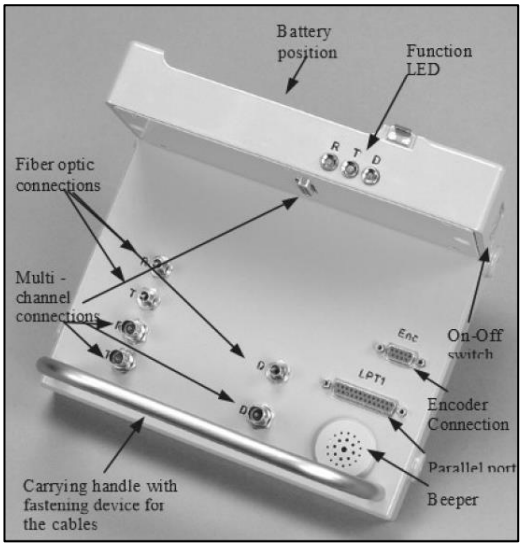

Fig. 4.1. MALA RAMAC CUII Control Unit

RAMAC CUII Specifications	
Pulse repetition frequency	10 - 200kHz (standard 100kHz)
Data bits	16
Number of samples/trace	128 - 8192
Number of stacks	1 - 32768
Sampling frequency	- 20 GHz
Signal stability	< 100ps.
Communications interface	IEEE 1284 (ECP)
Communication speed	>700kByte/s
Data transfer rate (from antennas)	40 - 400 kB/s at 4 Mbit/s
Acquisition modes	Distance/time/manual.

Internal computer	Motorola 683XX based at 25MHz.
Power consumption	25W
Power supply	8V RAMAC/GPR standard battery pack
Dimensions (CU II)	230 x 20 x 120 mm
Weight (excluding battery)	2.4 kg
Antennas and compatibility	All Ramac GPR antennas.
Maximum number of recording channels	4 or 16
Maximum number of antenna pairs:	MC-4 (2Tx & 2Rx) MC-16 (4Tx & 4Rx)

4.1.2. 1.6GHz shielded antenna

The antenna that we are using for this project is from the manufacturer MALÅ Geoscience, it is a dipole bow-tie shielded antenna with central frequency of 1.6GHz. It was designed for high precision quality surveys like concrete imaging, forensic surveys, layer thickness, and other applications that require high resolution in close-to-surface targets. It comes with a 4 meters optic cable that connects it to the control unit which is in charge of powering the antenna. A wheel cart with an odometer sensor will be connected to it to provide information about the antenna displacement. You will find below the specifications table for the antenna.

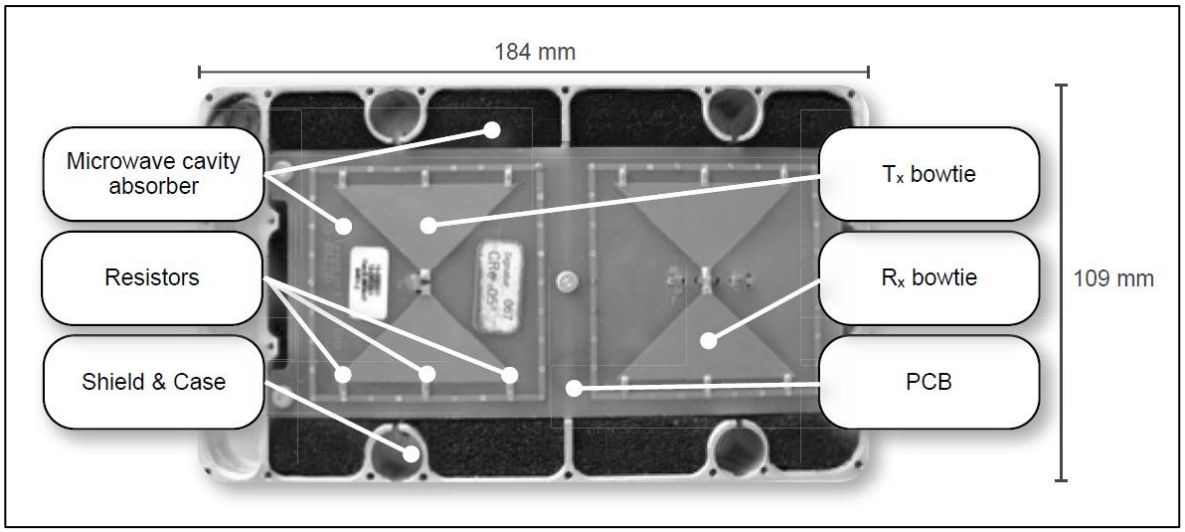

Fig. 4.2. MALA CX 1.2 GHz antenna opened with its parts defined. Which is similar to the antenna used on this work (the only difference are the dimensions) *Warren, Craig and Giannopoulos, Antonios. 2010.*

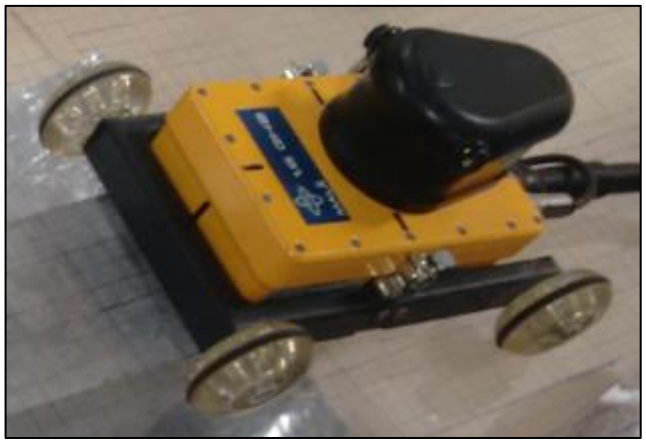

Fig. 4.3. Actual MALA CX 1.6 GHz antenna used for this project

1.6GHz shielded antenna Specifications	
Centre frequency	1.6 GHz
Bandwidth	> 100 %
Time window	> 50 ns
Repetition rate	100 kHz
Dimension	160x90x110 mm
Weight	0.6 kg
Cable length	4 m
Operating time	3 hours
Operating temperature	-20º to + 50º C
Control Unit	CX Main unit, ProEx or CUII control units
Data acquisition	CX Main unit or XV Monitor (both preferred) or other laptop (with MALÅ Ground Vision software)
Environmental	IP65
Options	Wheel cart, single wheel encoder, Extension handle, 10 m extension cable, split box for tomography applications

4.1.3. RAMAC XV11 monitor

The antenna and the control unit need a device that connect both, convert the signal from analogical to digital, stores the data, provide software, applies filters and adjust the parameters of data acquisition. In some cases, this tasks are carried out by a PC with an installed software, and it could be the case, the monitor RAMAC XV11 plays all this functions in order to prevent the user to take a PC with the equipment. With that being said, the monitor consists on an integrated software that allow us to modify acquisition parameters, visualize the data *in-situ*, storage the GPR files. In the front it has

Fig. 4.4. MALA RAMAC monitor used for this project

the power button, an LCD screen and a rubber button that can spin to navigate through the menus of the software. It has 1Gb integrated storage memory to store files and a USB port to connect an external device and extract data. It is powered by an external 12V battery with an average autonomy of 5 hours. The following table will provide information about the specifications of the device.

RAMAC XV11 monitor Specifications	
Power supply	Li-Ion 12V battery or other external source (9-18V)
Operating time	5 hours nominal (12V battery)
Operating temperature	-20º to +50º C
Environmental	IP65
Dimensions	326x215x52 mm (with protruding details 8.6 cm)
Weight	2.6 kg
Antennas	All MALÅ Antennas, except when operating the MALÅ Borehole Antennas in tomographic mode
Communication	Ethernet 100Mb/s
Display	Color backlit TFT LCD (640 x 480 pixels), trans-reflective (XV11)

4.1.4. GPR-SLICE Software

This software is used for processing and creating images of ground penetrating radar reflection data on this work. The Polytechnic University of Catalonia has the license of the software for Windows for the current year and due to its versatility and comprehensiveness is the chosen one to be the main software utilized in this project. It is compatible with lots of GPR manufacturer data, including the one for our project: MALA Geoscience. It was first commercially released in 1994 by Geophysical Survey Systems Inc. Later on, it was re-designed by the Geophysical Archaeometry Laboratory and adapted to Windows 2001 and it's been receiving periodic updates to improve its functionalities. We will be working with the version V7.0, commercialized by Geophysical Archaeometry Laboratory Inc.

5. Survey design and settlement

For the development of the tests, we would like to define a methodology and particularities for all of the tests that are going to take place for this work. As you already know, we are going to bury different objects in the ground and obtain GPR data from them in order to process them later and arrive to some conclusions about the efficiency of GPR data acquisition for 3D imaging

5.1.1. Location

The location was chosen based on the following criteria:

- The absence of underground obstacles like tree roots or big rocks, to avoid issues when digging. Holes were dug as far as possible from any tree, rock or building.
- Minimize the electromagnetic influence of other devices. So, Locations were far from electrical cables, laboratories, offices, etc.
- Totally horizontal terrain.
- Mediums with relative permittivity lower than 30.

With this parameters in mind, we chose 2 different locations: the backyard of EEBE school and the beach.

5.1.2. Field set-up

For the collection of data, we will be using an odometer attached to the antenna, this will record the path followed by the antenna and the distance recorded by the odometer will be the length of each radargram (x-axis). In order to generate proper 3D images, is mandatory to have parallel radargrams and so, the antenna needs to follow parallel paths.

As shown in 1.16. Section “Resolution between radargrams (range resolution)”, the best way to avoid aliasing and have best 3D resolution for dense gridding data without software interpolation, is that the sampling interval remains a quarter of the wavelength in the host material $n_x = c/(4f(\varepsilon_r)^{-2})$. If we take a look at the graphic (Fig. 2.13), the higher the relative permittivity is, the shorter the sampling interval must be. Having us a 1.6GHz central frequency antenna, the minimum sampling interval to ensure that almost every ground medium ($\varepsilon_r < 30$) can be recorded with dense gridding is slightly above 0.8 cm. Taking this into consideration, we will be recording all the data with a sampling interval of 1 cm to ensure and affirm that we will be doing dense gridding survey for all of our tests.

To ensure parallel data acquisition and the correct performance of the odometer, we took transparent acrylic 120x60 cm sheet and marked with parallel color lines spaced 1cm between each other creating a mesh. The material of the sheet is almost a perfect dielectric and although it may introduce some

surface continuous rebound of the signals sue to the air interface between the sheet and the soil, we can erase that effect later with the software. It must be commented, that the dimensions of the plastic sheet ensure that all objects buried will be easily surveyed and parabolic effect in radargrams will be fully recorded.

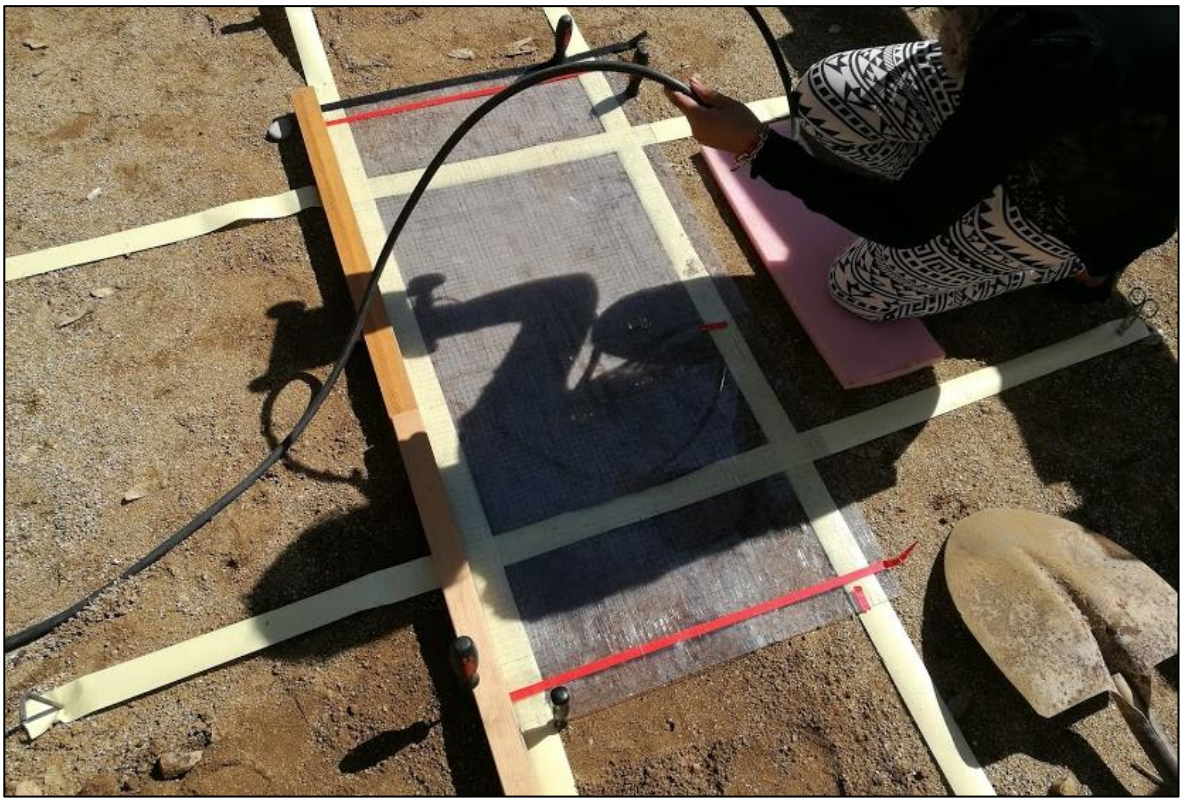

Fig. 5.1. Part of the field work

5.1.3. Data acquisition at EEBE

One of the locations for the acquisition of data will be carried out on the backyard of the Barcelona East School of Engineering, EEBE for the abbreviation in Catalan: *Escola d'Enginyeria de Barcelona Est*. This backyard is a soil based yard with some trees on it. The soil is clay type mixed with fine and very fine gravel. The reason for doing the surveys on this area is because the soil in this particular area suits for our requirements and we also avoid having to transport the equipment too far to other location.

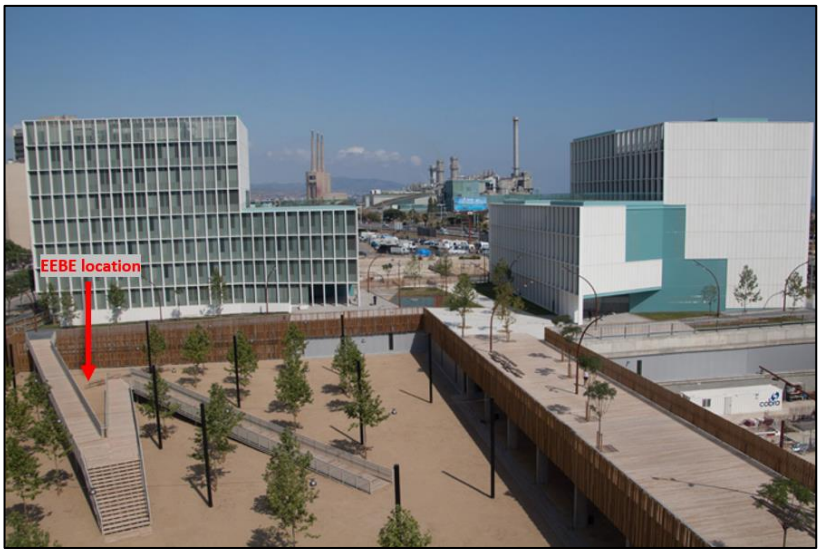

Fig. 5.2. Location at EEBE school yard

With the location for the survey in a small part of the backyard, he dimensions of the dig needs to be discussed. The depth of the hole was 20 cm, because deeper, the ground was formed of piedmont gravel, that introduces high porosity and makes very difficult to bury objects in.

The area for the hole will be a rectangle of 65x40 cm, an area wide enough to ensure that the targets can be buried easily. In addition, the sand will be compacted when the hole is plenty to ensure homogeneity and minimize the effect of the boundary of the dig.

Fig. 5.3. Details of the dimensions of the hole used to bury the targets at EEBE.

Having all that, the procedure for the acquisition of the data will be to dig the 120x60x50cm hole, cover with ground until the desired depth for the experiment , place the object of study and cover again with the rest of the ground, ensuring all the time the compactness of the surveyed area. Once the target is buried, the plastic sheet will be placed making coincide the target with the center of the shit. The next step will be to secure the sheet with different tool to avoid its movement.

The surveys carried out in EEBE where:

- Test 1: Metallic cylinder
- Test 2: Plastic tube and metallic tube in parallel
- Test 3: Three metallic plates at three different depths
- Relative permittivity determination of the soil

5.1.4. Data acquisition at the beach

For some of the tests, the beach was chosen to carry the surveys out. Fortunately, our school is very near from the beach, so the transportation of the GPR equipment was very short and easy. In addition, beach sand present a so many advantages that makes it a great location.

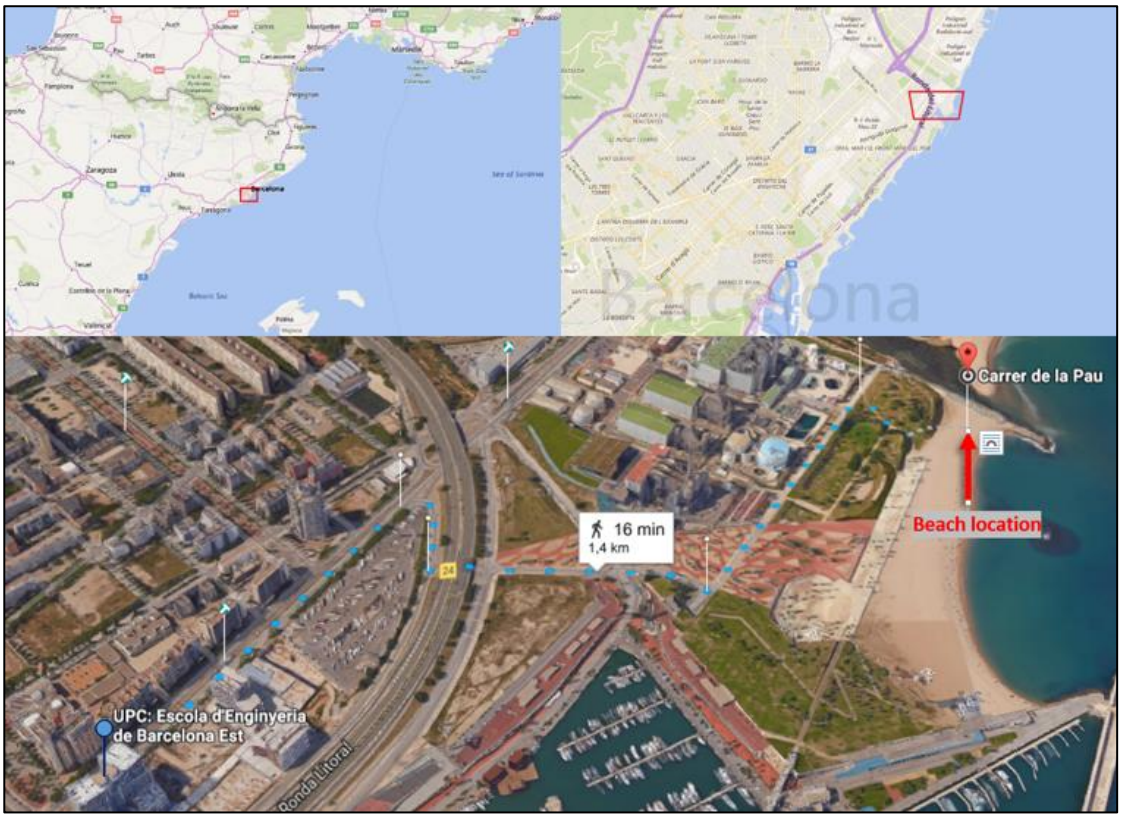

Fig. 5.4. Map of the location at the Forum Beach in Barcelona. It is 16 min far from the school by walk.

For this particular project, we chose the Forum Beach, located next to the Besos river mouth, in the Sant Adrià municipality and only at 16 minutes from EEBE by walk.

As we already mentioned, surveying in the beach present some advantages such as: easier digging process, easier way to compact the sand, higher homogeneity than other natural mediums or well-known medium in terms of electromagnetic properties.

Fig. 5.5. Picture of the set up for the experiments at the beach.

Experiments that where done in the beach are:

- Test 4: Hammer, metallic cylinder, wax sphere and metallic plate

6. Data processing

As explained before, the software that will be used for this project is GPR-Slice. On this chapter, all the post-data acquisition processes will be described from the very beginning until the final 3D model of the underground targets. This section would be close to a tutorial to help other people to create simple 2d slices and simple 3d volumes. I will follow the steps I made to get to the final data for the conclusions.

IMPORTANT NOTE: This chapter was built from my experience, and only describes a small part of the program. This is meant to add a different approach and source of information from a non-professional user to other non-professional users that want to use the software, and in particular, will follow the paths that I followed. The correct way to read this chapter should be to have it as the second or third source of information in order to learn how to use the software. With the software, an official user manual is provided and that should be the first source of information.

Introduction to GPR-SLICE

GPR-Slice is a folder-based software that works with different pre-set folders where the data is saved and overwritten. Different actions and settings done to the raw data will be saved on different folders and those folders (and the files inside) are editable from the Windows File Explorer. That allows the user to view, erase and transfer different steps of the data processing process, which is really useful, as lots of projects may require some user iterations and tries to arrive to profitable results.

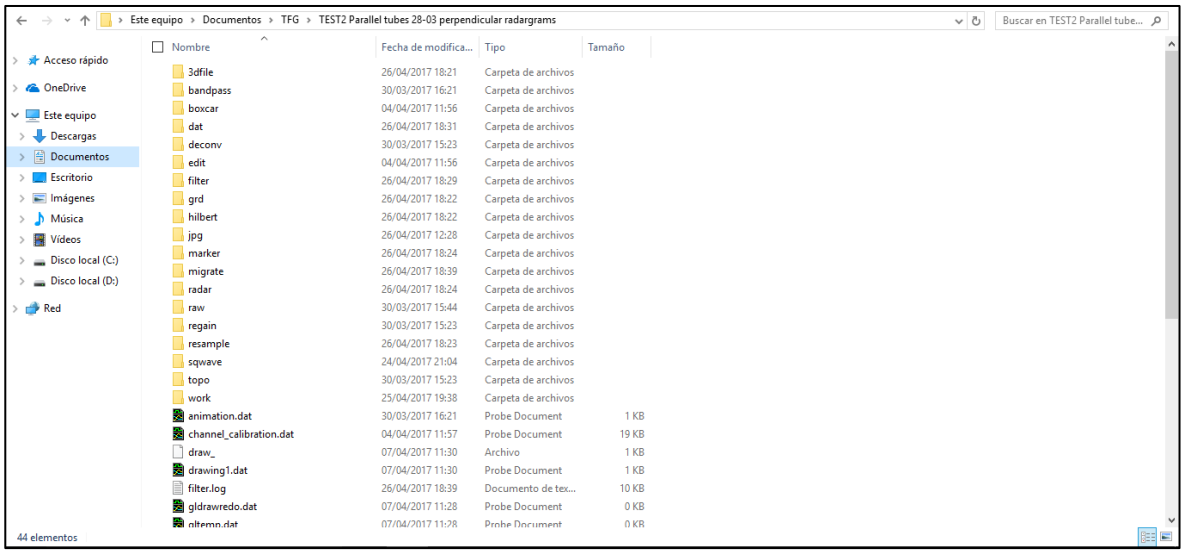

Fig. 6.1. Picture of the different folders created by the software by default

The software uses each folder to classify the file that are created during development of a project, that way, in different folders, data may have the same names but while there are located in separated

folders, the software is able to differentiate them. With that being said, folders should never be modified or some information may be lost.

At the beginning of each project the user will need to select a directory, where all these folders will be automatically created.

Create simple 2D time slices

6.1.1. New project & Transfer data

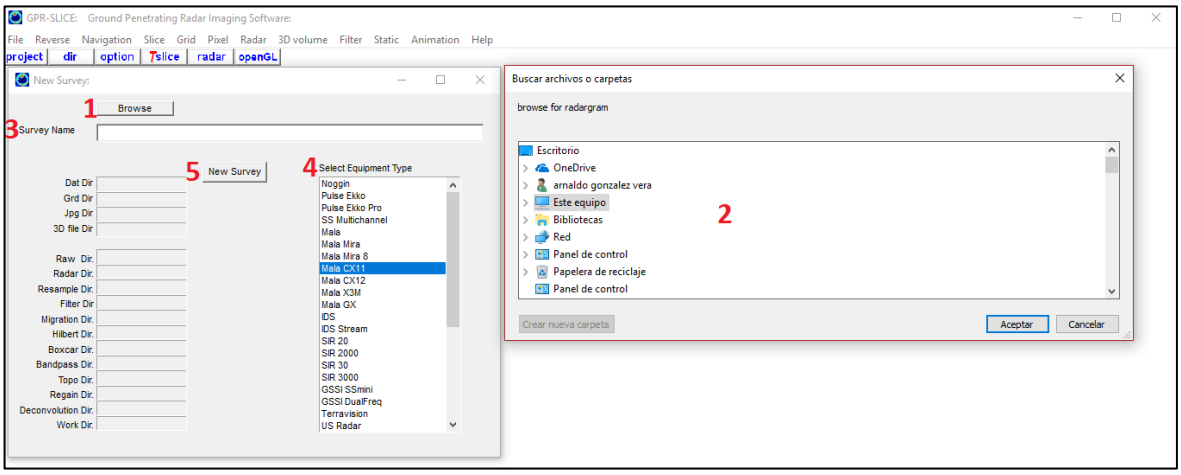

Fig. 6.2. Screenshot of the first steps to create a project in GPR-slice

The first step to begin a work in GPR-Slice will be to click File on the Menu Bar, and then New project. A new window will be opened, and the user will need to specify a directory, a name for the project and the type of the GPR equipment.

When the location of the project is set, the raw data acquired on field needs to be uploaded to folders. Clicking on File, transfer data a new window will be opened. On browse button, we need to specify the directory where raw data is, and then click the button search to let the software find the GPR data on the selected folder. On the "file type" field, we recommend you to set "." In order to let the software find all the files related with GPR. However, you might select another file type depending on the manufacturer. Finally, click on import radargram data \raw\ folder to save the filed data on the raw folder.

6.1.2. Create new info

Radargram files are usually named as a unique identifier (e.g. "DAT_"), a number that is correlative and each radargram has its own (e.g. "1234") and an identifier (e.g. ".rd3"), resulting, for example,

"DAT_1234.rd3". For the next step, click on File and create new info. Here, the user needs to specify the total number of radargrams on # of files, (advice: when setting the number of files, count all the correlative radargrams, including the invalid ones that you may have, because they can be deleted later). The file identifier field is preset when the user selected the equipment type, so you may not need to change this. Ending identifier is also preset by default.

As we explained before, radargram files had a number that identifies them (DAT_**1234**.rd3), on the field name increment, the user must indicate how the identifier number increases between correlative files (for example, if we had two files DAT_**1234**.rd3 and DAT_**1235**.rd3, the name increment should be 1). Name start indicates the first file for the software to start counting.

Below, mark how the radargrams where taken: Parallel to the X axis, parallel to the Y axis, an XY grid, with different angles, following a GPS signal or defining a vector. After that, specify the dimensions of the measures according with the checkbox marked before. We recommend the user to draw a plane specifying lengths and of the files to avoid confusions. By default, the software works with meters, however, the user can change this on the menu options.

When all the information has been set, click on create info, and close the window.

6.1.3. Edit info file

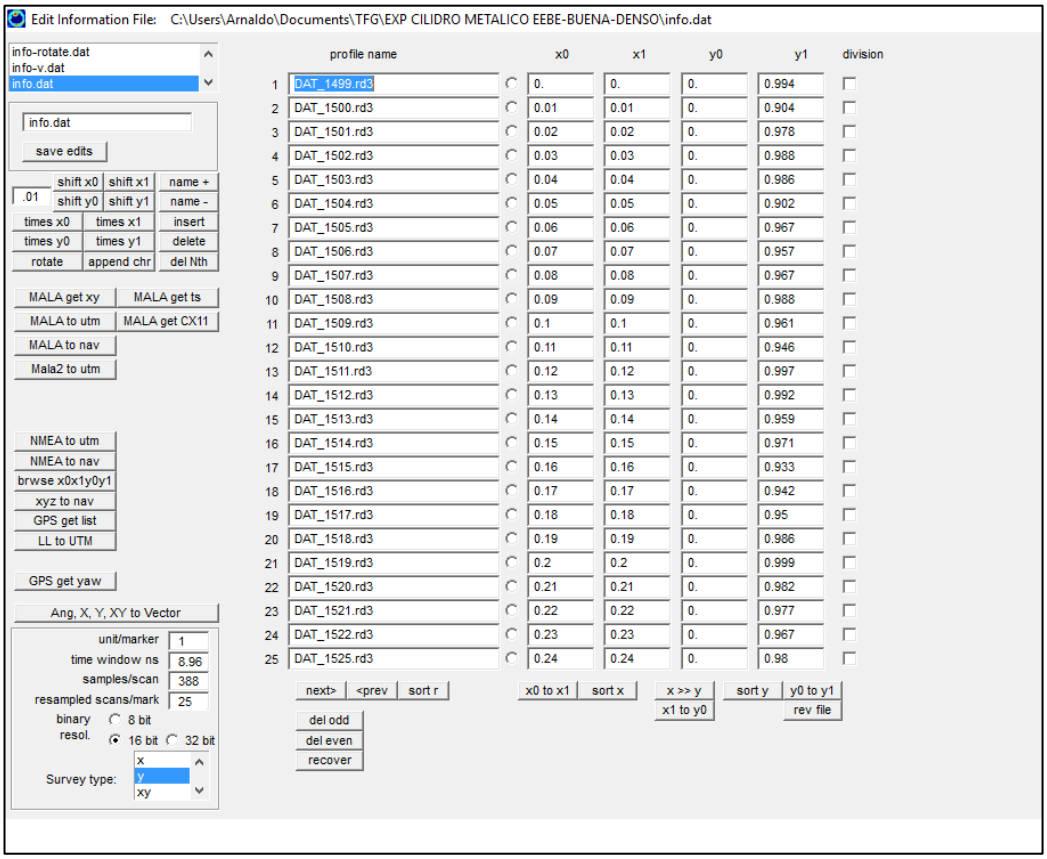

Fig. 6.3. Left, there are the different buttons and options (remind that "MALA get xy", "MALA get ts" and the other buttons in which states "MALA", is because we chose MALA for the equipment type). Right there are radargram names along with all its measurements and position.

File, edit info file to get to the next step. On this window, the user will see all the uploaded files according with the information set before. As recommended before, in case that the user had some invalid files, this menu allows to delete invalid files as well as other editing options. Let's start in case that the user needs to erase invalid radargrams: next to the profile names, there is a check box, mark the file to be deleted and then click on delete. When all the files shown on this window are valid, next step would be to specify the lengths and spacing between them. The user can change all the values manually on the four columns "x0", "x1", "y0", "y1", nevertheless, we strongly recommend the user to use the option brwse x0x1y0y1. This option allows the user to browse for an external .csv file containing the information of x0, x1, y0, y1. The file to be uploaded needs to have as much rows as files the user have and only one column; the values need to be separated by commas and in case of decimals, use the dot. The user can easily create this file on excel and then upload it clicking on brwse x0x1y0y1.

On this menu, there are lots of different options and combinations because different buttons appear depending on which "equipment type" we selected. We recommend the user to check the user

manual, as this software supports lots of different GPR manufacturers. In addition, my experience doesn't allow me to explain the various buttons properly.

When all the necessary changes has been done, click on save edits, to store the changes.

6.1.4. Convert Data

The final step to have the radargrams ready to process is the "Radargram Conversion". Radargrams collected by the different manufacturers, needs to be converted to GPR-Slice format, and usually, raw data is collected without any kind of gain or pre-set conversion, so this is also helpful to make easier to the user (and the program) the visualization and process of the radargrams. Click on File and convert data. A new window will pop up, to begin the conversion click on MALA 16 to 16 bit (notice that the text "MALA 16" will change depending on the manufacturer and the equipment, this is just an example). The new menu will have on its center 4 different diagram giving certain information. Starting from the left, the first diagram represents gain against depth (in ns), the second is the selected

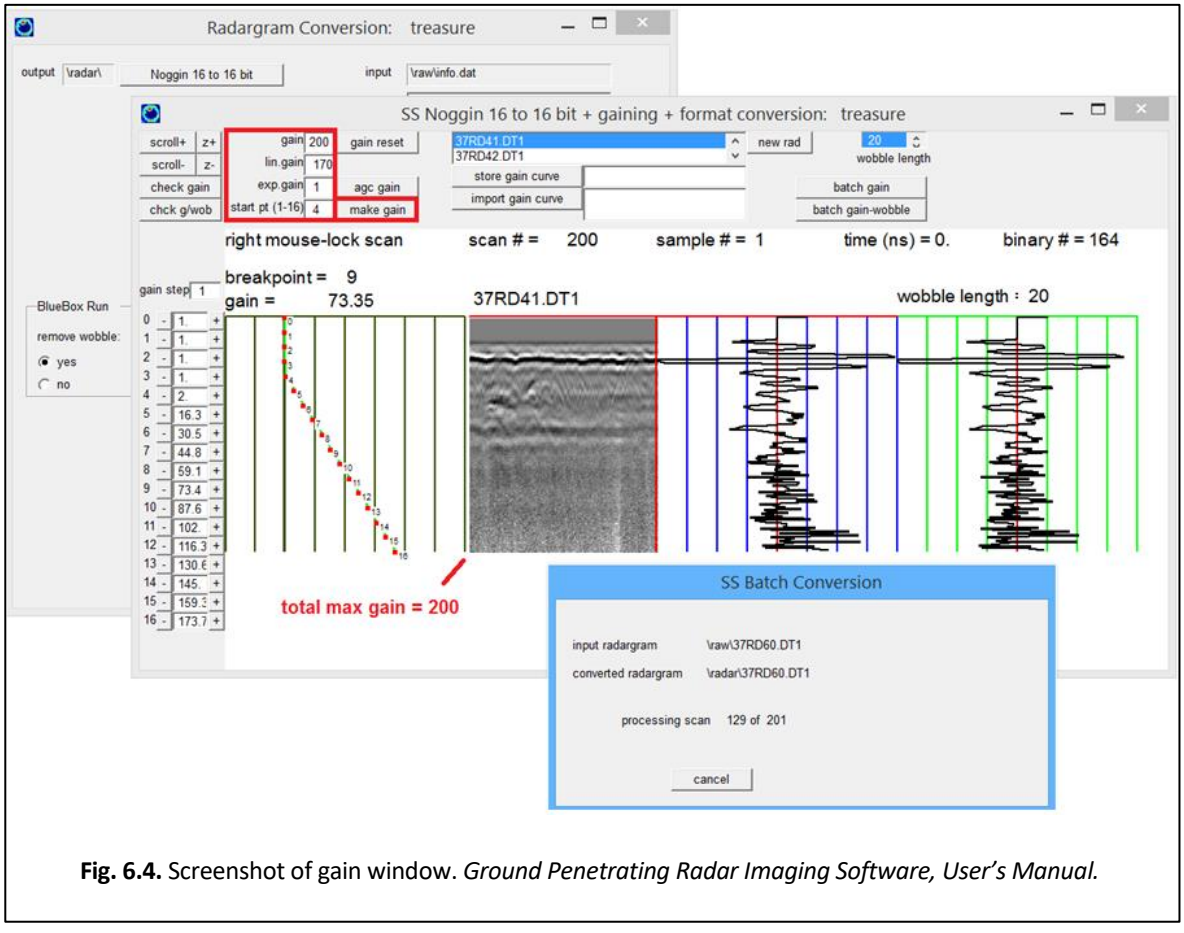

Fig. 6.4. Screenshot of gain window. *Ground Penetrating Radar Imaging Software, User's Manual.*

radargram for the user to view (the user can change which radargram is shown selecting the desired file and clicking on new rad), the third diagram represents the gained amplitude against depth for every scan of the radargram (moving the mouse over the radargram, the software will represent amplitude

for every scan), the diagram on the right represents the amplitude against depth for every scan of the converted file including gain and dc-drift subtraction of the gained files.

As we mentioned, the user is able to modify the gain on the radargrams as desired; this menu, has various ways to modify the gain curve to be applied to the files. The diagram on the left, representing the gain by 16 dots along all the radargram depth, can be manually modified by the user by clicking on each dot and changing the gain to suit the desired result. In addition, the gain on each dot can be typed by the user to the desired value. The idea is to create a curve that enhances the targets and tones down the noise. The software also has the possibility to create an automatic curve typing a value on "lin.gain" (linear gain curve) or either "exp.gain" (exponential gain curve), then setting a maximum gain value on "gain", selecting an starting point for the curve on "start pt (1-16)" and finally clicking on make gain. <<The exponential gain curve would further gain faster with depth to a value of (exp(i/z)-1) where i is depth along the scan and z is the total depth. The value of 1 is subtracted such that if exponential gain is turned off, the total exponential gain contribution is 0>>. (Ground Penetrating Radar Imaging Software, User's Manual)

In addition, the user can click on agc gain to let the software create an automatic curve based enhancing lower reflections on radargrams. Remind that if the automatic curve doesn't suit to the the user it can be changed by using the tools explained before. The button gain reset readjust the gain curve to its default value (0). Finally, there is the option to store the created gain curve by clicking on store gain curve to be able to import it later (or for other projects) by clicking on import gain curve.

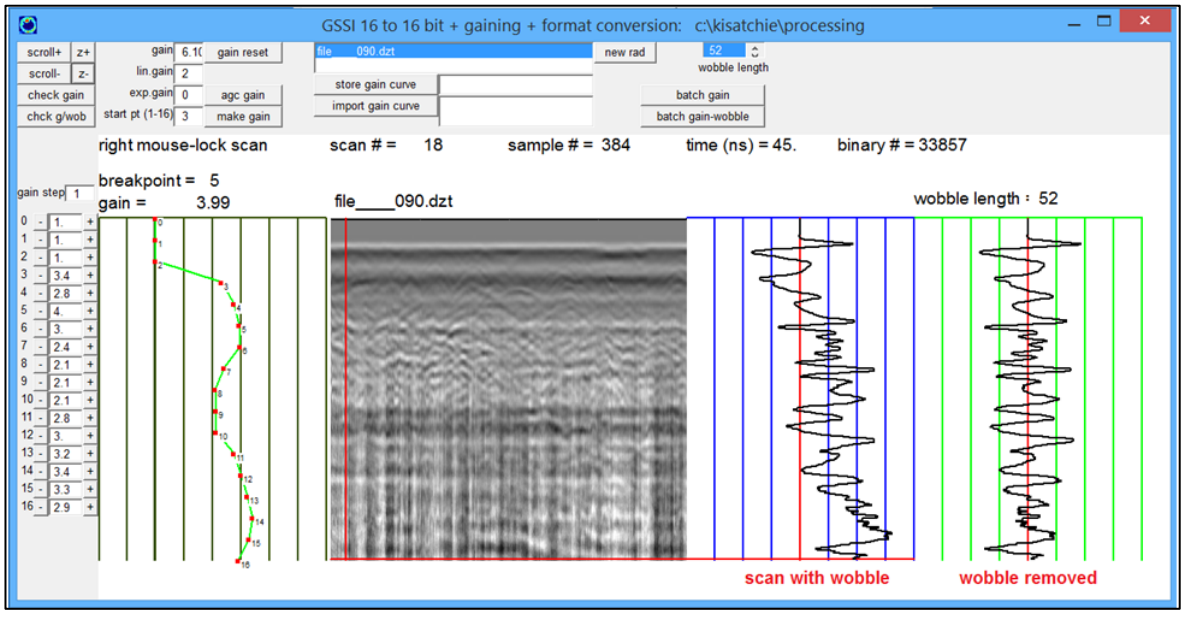

Fig. 6.5. Screenshot of gain window. Notice the signal with wobble removed. *Ground Penetrating Radar Imaging Software, User's Manual.*

When the user had done the desired changes, the button batch gain will apply the gain to all files and the button batch gain-wobble will apply the desired gain plus a dc-drift substation (possible to see on the diagram on the far right).

6.1.5. Reverse

In case that the radargrams had been taken in different directions and the user desires to reverse them or switch the direction of some of them, this menu will help for this purpose. Click on Reverse and then, reverse to open the reverse tool.

Next to each radargram name, there is a checkbox used to select the radargrams that the user wants to do the reversion to; select the radargrams desired to be reversed and then the software provides various buttons for different selection patterns. Odd will mark odd radargrams starting with the first on the list, even will mark even radargrams starting on the second, all marks them all and none unmark them all. Additionally, there are four more buttons: even name, which will mark radargrams with an even identifier, odd name (same, but with odds instead). Even interval will tag radargrams that, given a certain profile interval, are positioned in even positions of the mentioned profile interval (for example, if spacing between radargrams is 0.15m, and radargrams are positioned in 0.15, 0.30, 0.45, 0.60, 0.75, 0.90…, this will mark 0.30, 0.60, 0.90, etc.); following the same logic, odd interval will mark odd positioned radargrams.

In case that needed, the user must reverse the desired radargrams. An example from my experience is that this can also be useful, even if radargrams were obtained following the same direction, because the software may take the end of the radargrams, as the origin. When aligning radargrams with slightly different length, they don't fit and distortion the final image, so reversing them all solves the distortion, as the origin of the radargrams is the same as the start. It is also recommended to take strong field notes in order to avoid any confusions when working with the software.

6.1.6. Navigation

Set navigation is the next step on our way to create simple 2d time slices. To access to the new menu, click on Navigation and then markers. Markers are reference points added along all the radargram length, which the software uses later to create time slice, 3D volumes and other elements. Sometimes, markers are added on field by the GPR equipment or a GPS equipment, but sometimes markers need to be added by the software (it will depend on your equipment and configuration).

We can find four main buttons on this window, Artificial Markers are markers automatically added by the software, and this should be the option to take if the user has done the survey with an odometer wheel (which is our case). Field Markers, add markers that were created on the field by our GPR

equipment and this should be your option if you had configured your equipment to this purpose. The button Interval Markers, add markers every certain quantity of scans as the user desires to configure on the textbox below. The fourth button GPS/Vector Trace#, inserts markers if you had a GPS equipment and it recorded markers along the radargrams.

Notice that, the software will overwrite markers when you click one of the buttons, save the markers that where at last inserted. So in case of having field markers, if one clicks on Artificial Markers, the field markers will be overwritten.

Before clicking on Artificial Markers, ensure that the checkbox "MALA survey wheel" is marked, as we had used an odometer for this survey. Remember that MALA is the equipment type used on this project and thus, all the options shown here are referred to this equipment type. If the user have a different GPR equipment, names will change, but the buttons will have the same function.

The user also has the option of viewing each of the radargrams with the markers added on the step before if we click on Navigation and show markers.

6.1.7. Slice

This is the final step to obtain our time 2D slices, when we finish this step, the only feature to learn is how to visualize the 2D time slices. First, click Slice on the menu bar and then slice/resample to open the slice configurator. You will see three differentiated parts on the new menu: a bunch of buttons and textbox on the left, a central overview of the information of the time slices and a squared board with information about the process history on the right.

Before going for the step by step process, is interesting to understand how GPR-Slice manages slices, and how it creates them in order to understand better which changes are we making on the slice menu. Basically, if radargrams are 2D vertical representations of the soil, slices are simply software-generated 2D horizontal representations of the soil, based on the information provided by radargrams. Simplifying the process, GPR-slice split the radargrams in various fragments by different depths, then takes all the fragments of the same depth and combines them by different interpolation processes, managing to combine the divided parts and resulting to create horizontal 2D representations of the soil.

Let's start with commands of the left side. On top, the user needs to choose where to create the time slices from, that is, which folder the software would pick to take radargrams and create the time slices. From now, we haven't saved any files on any folder but "\radar", so we will choose \radar folder (if the user desires so, slices can be created from a different folder, for example, from the folder \filter after a background removal).

Below can find a bunch of textboxes to type in and some buttons. The first thing to do is find the real 0ns of our measures. When we place our GPR equipment directly upon the ground, the first emitted EM waves bounce between ground surface and the surface of GPR equipment, producing that the first recorded signals (first nanoseconds) of our radargrams are just continuous reflection of the EM wave. We need, then, to find where the real 0ns of our measures is (Ground Penetrating Radar Imaging Software, User's Manual).

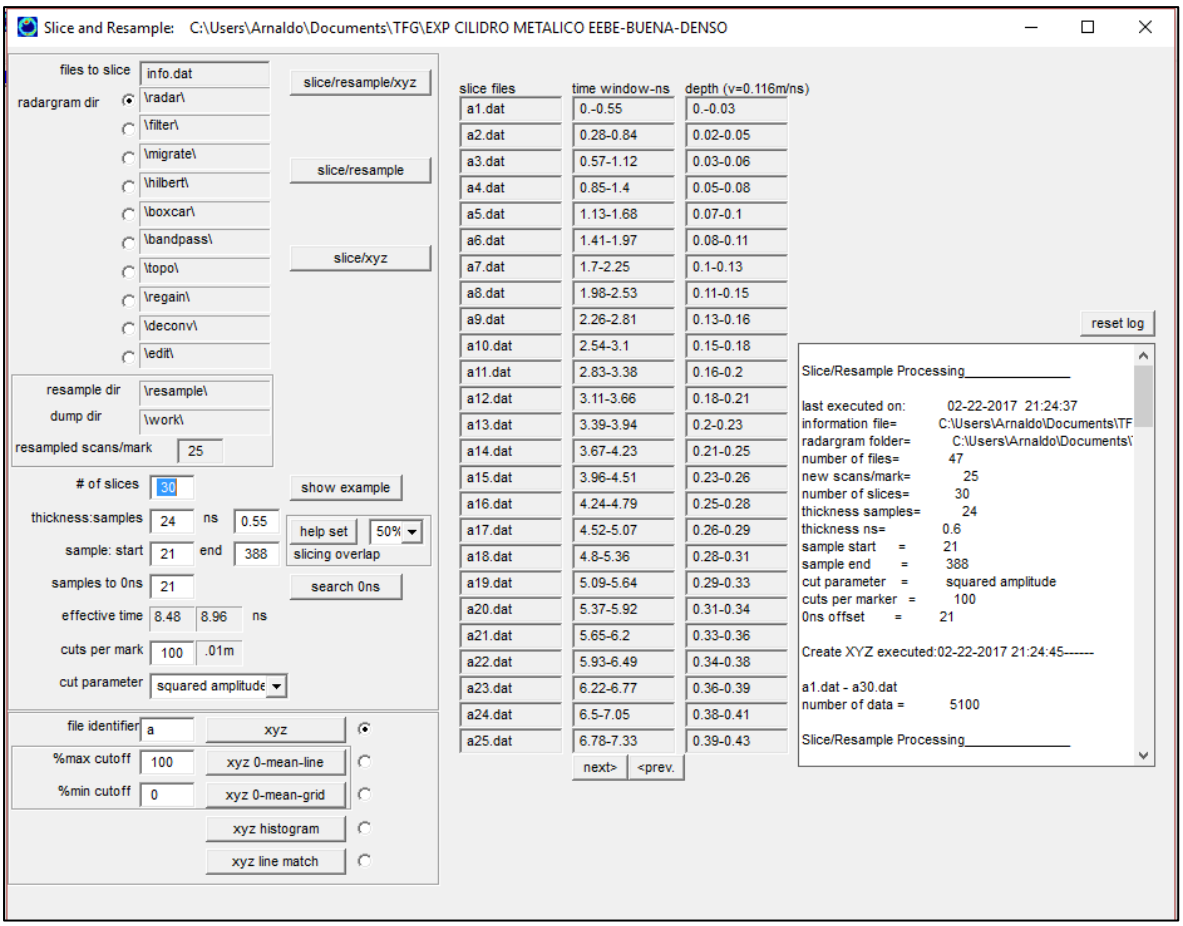

Fig. 6.6. Screenshot of Slice window.

Click on search 0ns to open a window with an illustration radargram to choose and then the user needs to click on the part of the radargram where the 0 ns is. This can be easily done with some experience, but if you are an unexperienced user, click on auto-detect to let the software find it by itself. When the 0ns is detected, close the window and start with changing the different parameters to have the slices done.

First of all, select the desired number of slices on "# of slices". A high number of slices, will provide a better representation of the soil, but will make the rendering time so much longer; on the other hand, a low number of slices, won't allow the use to represent the soil properly. In our case, we are typing

30 slices, which combined with the overlap and the thickness of them, provide a pretty good resolution. The “thickness:sample” and the “slicing overlap”, are the other parameters to take into consideration. For the slicing overlap, we recommend to always have an overlap value (50% in our case) to reduce the

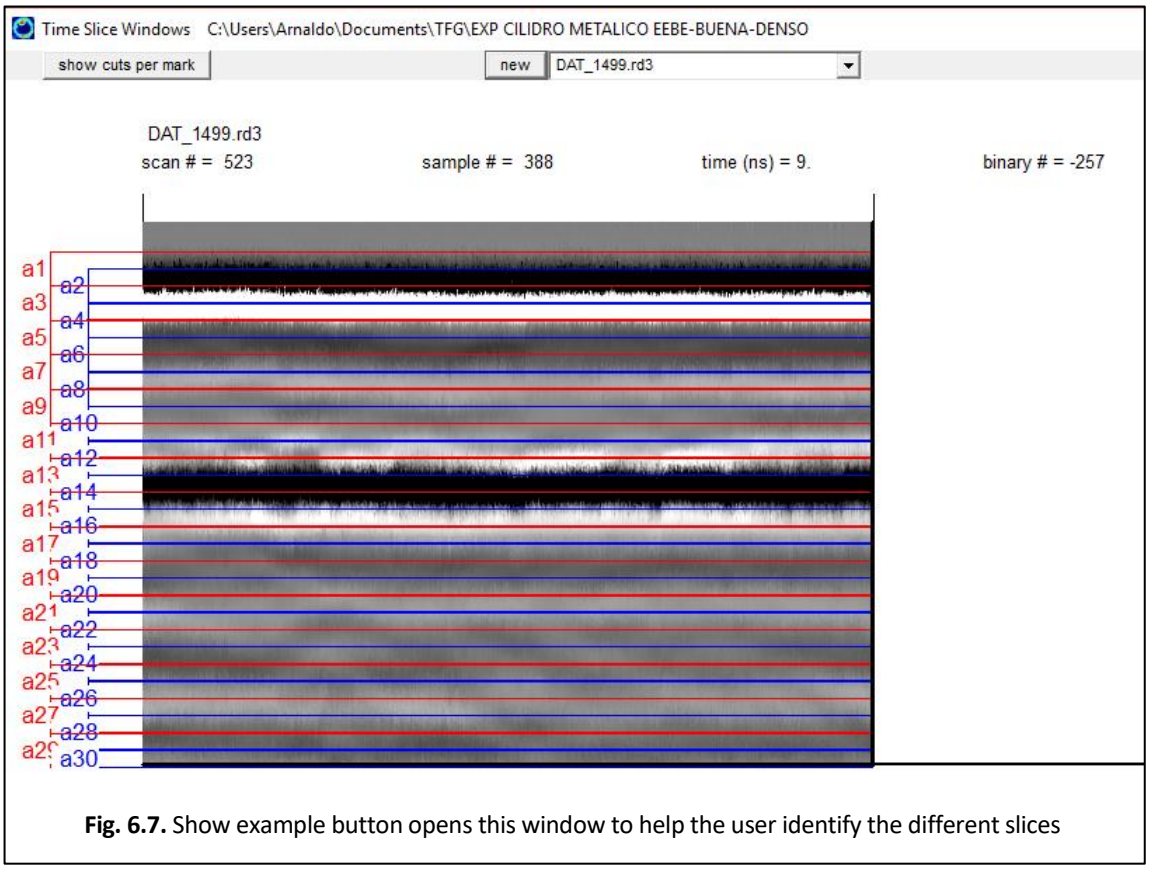

Fig. 6.7. Show example button opens this window to help the user identify the different slices

loss of information to a minimum , which means that every slice will always pick information from the slices above and below, resulting a much better representation of the soil, as when the software interpolates, a lot of the information is lost.

The “thickness:sample” is how many samples does each slice measures. If the user desires high resolution, a short thickness is advised but it will augment the processing time and on the contrary, coarser slices will provide worst resolution but the processing time will be shorter. The user can change the “thickness:sample” either specifying the number of slices or the nanosecond for each slice. Changing one of those text boxes will automatically change the other. Clicking on help set will automatically adjust the slice thickness for the number of slices and the desired overlap.

For the user to be easier to visualize the slice disposition and measures, click on show example. “Sample start” is at which sample the 0ns is located and the “(sample) end” is the last sample which the software will take to create the slices.

For the other options in this menus, we address you to the user manual for a deeper view of all the functionalities.

Finally, the user needs to choose one of the three processes that the software provides: slice/reample/xyz, slice/resample, slice/xyz. Slice/resample/xyz will create the slices by interpolating between radargrams to complement the information of the radargrams and will create a 3-dimentional box based on the length and space between radargrams, where a 3D volume can be created later. Slice/resample will also interpolate between radargrams but won't crate the 3-dimentional box and in order to create a 3-dimentional volume, further actions need to be done later. Slice/xyz will create the slices without any interpolation between radargrams and will generate the box mentioned before. The question is, which option is the best and in which situations is advised to take one or the others.

Slice/resample/xyz and Slice/resample is the option when the spacing between radargrams is more than a quarter of the wavelength, in other words when the gridding of the survey is not dense (for more information go to chapter "resolution between radargrams (range resolution)"). Typically, when the spacing between radargrams does not allow to perceive all the information down the ground, this is the best option because software will interpolate what is between each radargram and will "complete" by itself the missing information caused by the large spacing between each radargram. This option is the optimal for large extensions of soil and is typically the case of archeological surveys.

Slice/xyz won't interpolate (or resample) between radargrams, so this will be the best solution when the distance between the radargrams is not too big because there is no need to interpolate the information between radargrams, as radargrams are so close that all the information is acquired properly. Typically, for civil engineering this is the best option, since it is more likely that the surface of survey is shorter than in archeological studies and radargrams are closer.

Click on the desired button and wait for the software to process. In our case we click on Slice/xyz.

6.1.8. Grid

In order for the software to finally create the time slice, we need to click first on Grid on the Menu bar and the click on grid. A new window will open with different options to modify and process slices that we recommend to read on the user's manual because there lots of combinations and variations. We are only focusing on "X grid start", "X grid end", "Y grid start", "Y grid end", which are basically text boxes to define the space box where slices will be represented in. For example, if the user wants to only represent the slices on half of the radargrams, the user should change the values in order to set the measures of the slices. There is also the option to define the size of the grid of every slice, basically is the measures of the pixels of the slices, bigger "grid cell slice" will make the resolution of the slices be worst that a smaller value for "grid cell slice". When the user has set all the desired values, click on start gridding and the software will finally create the time slices. If the option of "processing graphics" is checked, the user will see the slices at the same time as the software processes them.

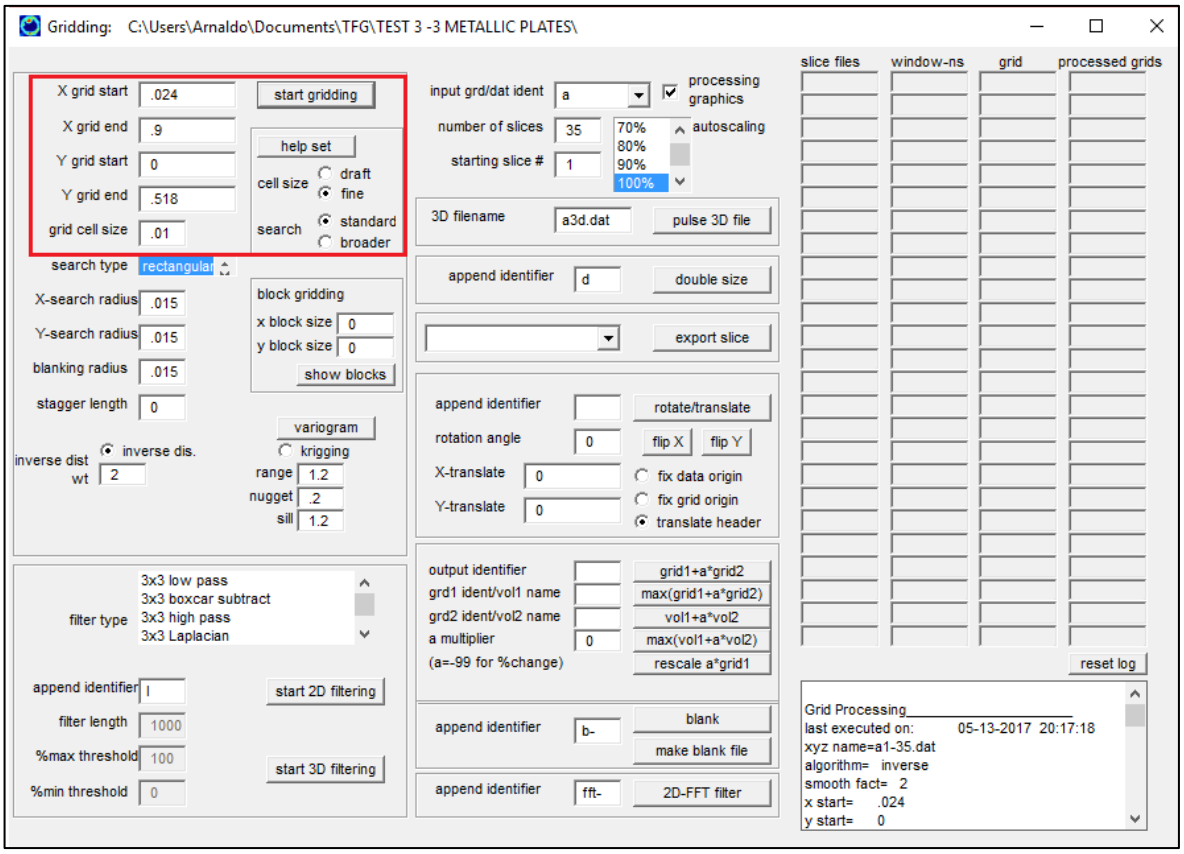

Fig. 6.8. Grid window. For this tutorial we are only focusing on the marked space.

7. Tests description

Test 1: Metallic cylinder

This was the first test carried out at EEBE facilities. We not only used this test to acquire substantial data to this work, but also for testing out the equipment and testing the software, as it is a very simple experiment. We placed a metallic cylinder at the middle of the hole at 20 cm depth, the dimensions of the cylinder are 11cm of diameter and 2.5cm height.

Radargram direction are shown in the following image

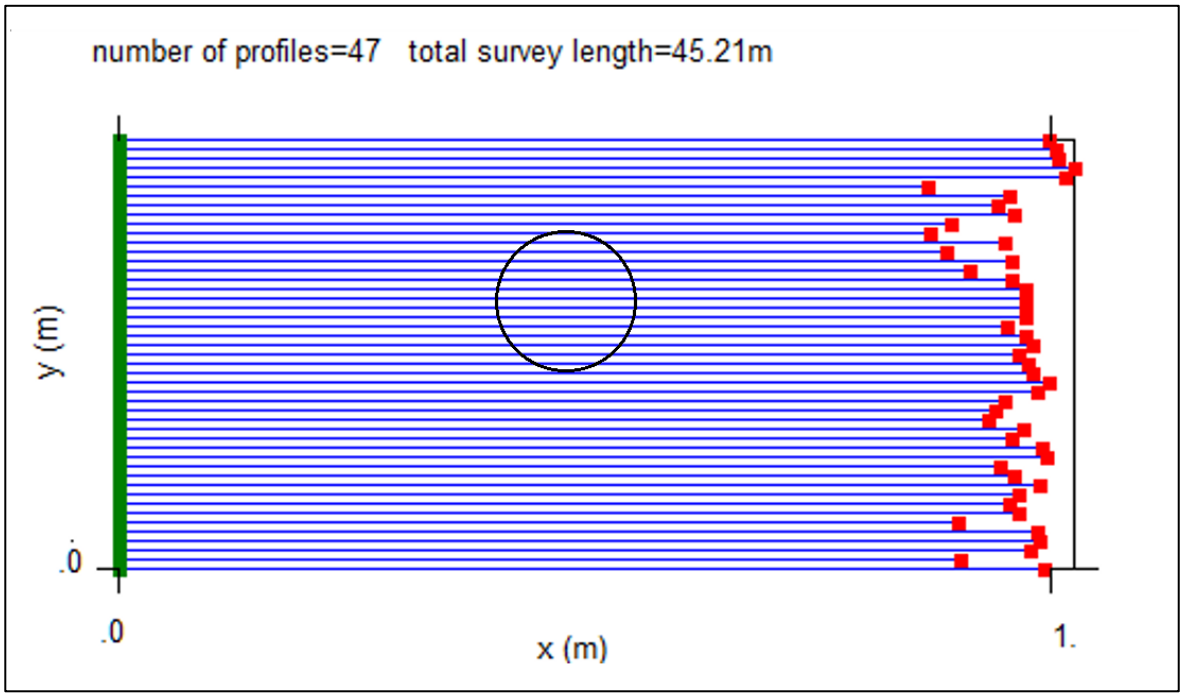

Fig. 7.1. Grid plot from GPR-Slice, which represents radargrams directions and lengths.

Test 2: Plastic tube and metallic bar in parallel

The objective of this test is to simulate underground pipe's conditions and represent them with 3D GPR software. Both tubes were the same size, however one made of metal and the other made of a plastic material. The one made of plastic was

Sizes:

- 4 cm of diameter
- 50 cm length

- 1.5 mm thick (only the plastic pipe)

Placement:

- Placed in parallel
- 21 cm between each other
- Plastic pipe at 17 cm depth
- Metallic pipe at 15.5 cm depth

Fig. 7.2. Details of the position of test 2 objects.

We performed two different radargram directions for this test in order to see what the implication of radargrams direction is. Perpendicular to the tubes and parallel to the tubes. See the following image for further details:

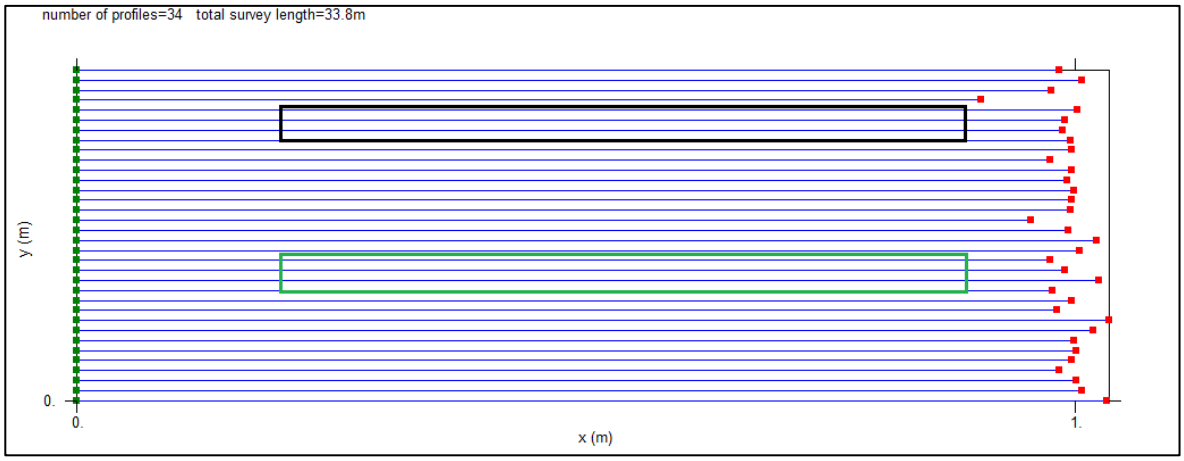

Fig. 7.3. Grid plot from GPR-Slice, which represents radargrams directions and lengths

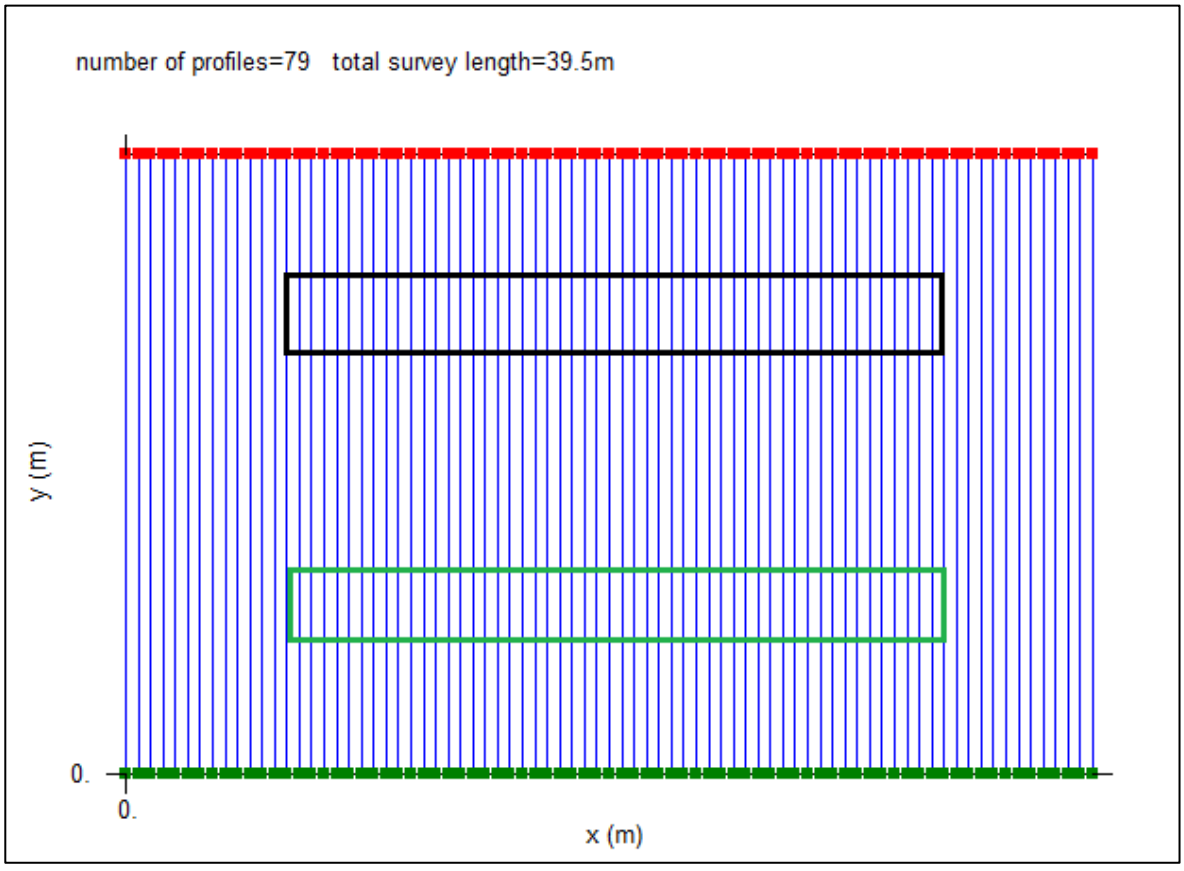

Fig. 7.4. Grid plot from GPR-Slice, which represents radargrams directions and lengths.

Test 3: Three metallic plates at three different depths

The objective of this test is to find an experimental correlation between depth and size of the target when it comes to resolution. The three metallic plates where made of the same material and had the same size:

- 20 cm length
- 5 cm wide
- 3 mm thick

Placement:

- One plate on each depth
- 20 cm
- 13 cm
- 8 cm

Fig. 7.5. Details of the position of test 3 objects.

Regarding the direction of the radargrams, we follow the direction parallel to the plate's long distance. See the image below for further details:

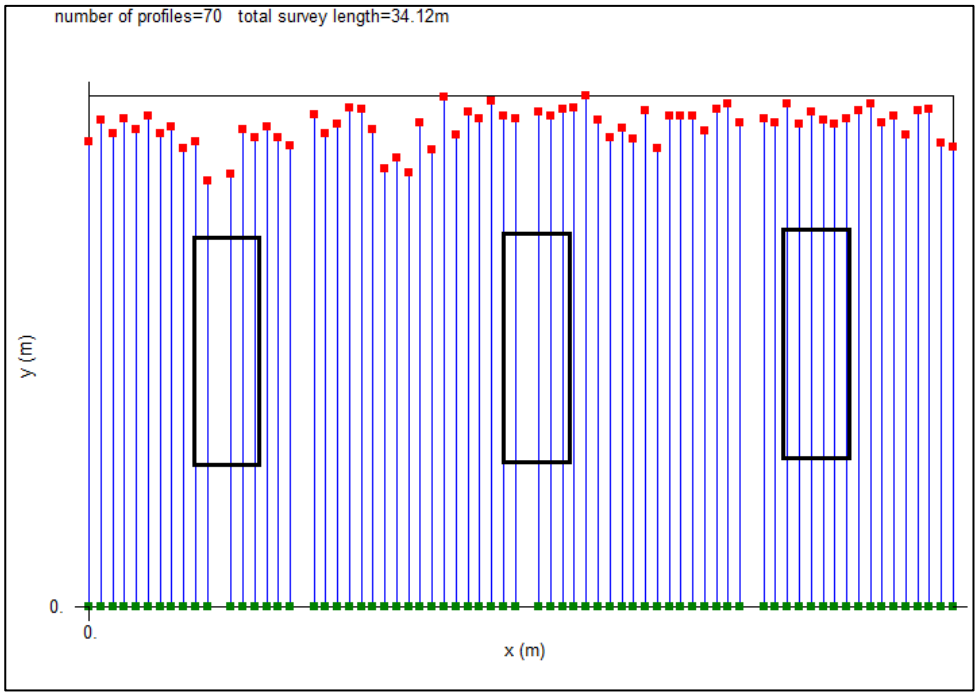

Fig. 7.6. Grid plot from GPR-Slice, which represents radargrams directions and lengths.

Test 4: Hammer, metallic cylinder, wax sphere and metallic plate

The objective of this particular test, is to compare the resolution of each objects when different materials are set in the same area, as it is usual in non-controlled surveys. This experiment seem to us very interesting, because in the same study, we have lots of different studied variables going on: different shapes and sizes, different and much differentiated materials (metal, rubber, wood and wax). As well, the fact that the rubber and the wood are touching, and they had a cylindrical shape (just as a pipe), along with the sphere, which is made of a slightly reflective medium and the metal shapes that are placed different from previous experiments makes this experiment so rich and interesting.

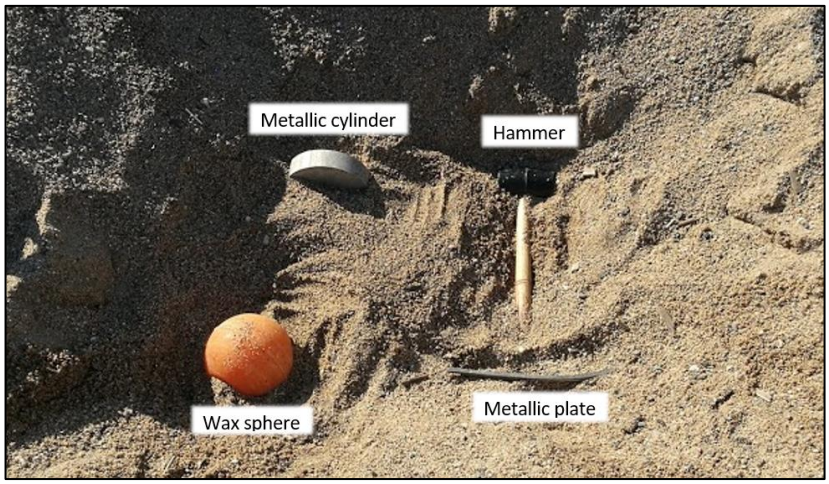

Fig. 7.7. Details of the position of test 4 reflectors.

For information about the radargrams direction, please see the image below:

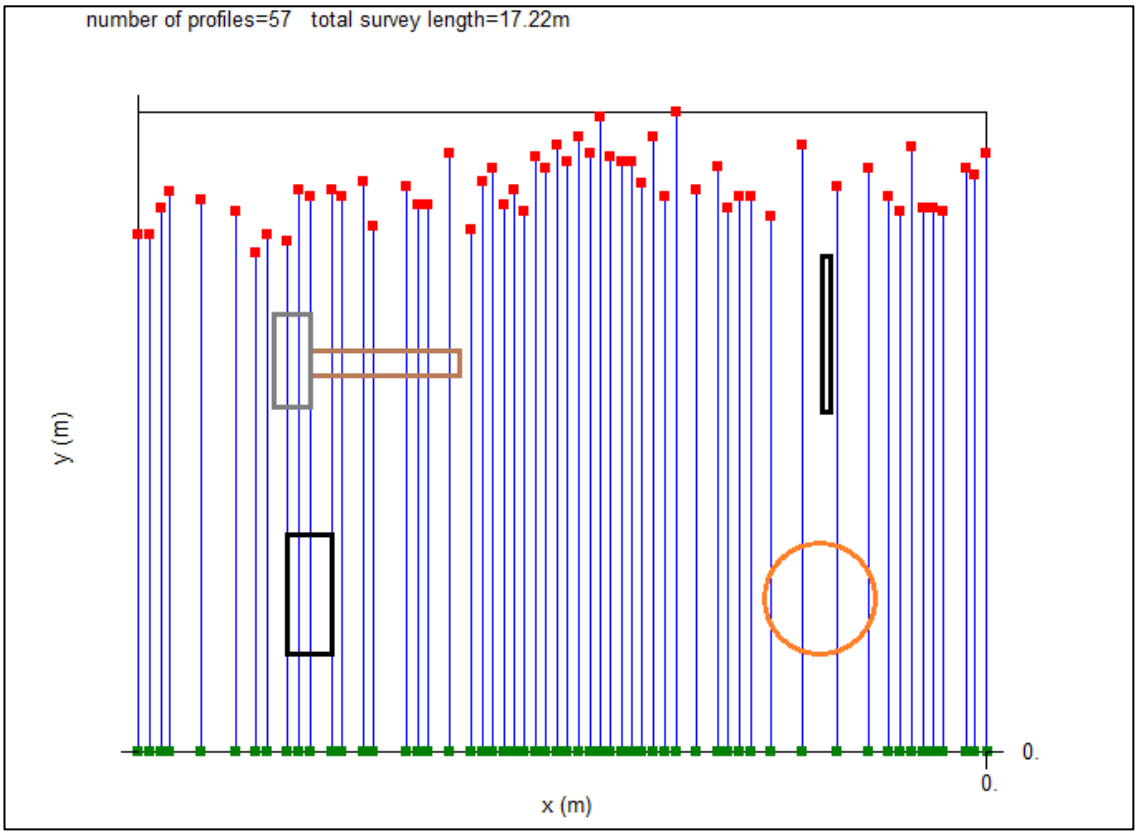

Fig. 7.8. Grid plot from GPR-Slice, which represents radargrams directions and lengths.

8. Results and conclusions

Finally, one of the latest chapters of this work. On this section, we are going to describe the results obtained from the tests based on the theory and the applied process to get to the results and then go for the conclusions of each test. Finally, we are going to sum up all the conclusions for an overall view.

From Test 1

This was the first valid test of this work after some adjustments and failed tests and it is very special because is also one of the tests that I have worked more with and used to learn how to use GPR-slice and its functionalities. The results are arguably successful because after the process, we can observe the cylinder represented in 3D with a reasonably good resolution taking into account some the factors that we will discuss now.

To get to the final 3D representation of the metallic cylinder, first, we acquire radargrams every 1 centimeter, then we processed data applying a bunch of filters provided by the software. First filter to be applied is one of the most used filters: Background Removal, which eliminates the average scan across the radargram from each individual trace and basically is used to subtract noise across the radargrams. After Background Removal, next filter was Migration, which basically, sums up every part of the hyperbola that appears on radargrams due to the behavior of the electromagnetic waves when they reflect an object.

Different filtering processes generate variations on the final 3D volume shape as the volumes are generated based on variations of the amplitude and when applying the filters, we alter amplitudes, making the final volume change its shape.

On the other hand, we have find out something very interesting regarding the spacing between radargrams. Theory tells us that in order to have the best resolution, we need to have a dense gridding survey, which can be defined as the maximum distance that radargrams need to be spaced between each other (sampling interval). This distance can be calculated as a quarter of a wavelength (chapter "Resolution between radargrams (range resolution)"). However, for this particular work, we have noticed that having an ultra-dense grid survey does not always make the shape of the 3D volume be as accurate as it could and we are going to show that effect on this section theoretically and with the 3D volumes obtained from different spacing between radargrams.

For this test, the sampling interval to perform a dense gridding survey is defined as:

$$n_x = \frac{c}{4f\sqrt{\varepsilon_r}} = \frac{75}{f\sqrt{\varepsilon_r}} = \frac{75}{1600\ MHz \cdot \sqrt{6.81}} = 1.8\ cm$$

Relative permittivity calculated on from the actual radargrams with equations showed in the theory part.

On the field, we acquire data with a sampling interval of 1cm, so the theoretical sampling interval is by far covered. Keep this in mind, because we will go back to this in a moment.

Now, checking the theoretical horizontal resolution of our GPR antenna, which basically tell us is the equipment is capable of distinguish two different reflectors at the same depth as two different events. There are various equations from different authors:

$$\frac{d}{2} = r = \frac{\lambda}{4} + \frac{z}{\sqrt{\varepsilon_r + 1}} = \frac{2.75cm}{4} + \frac{20cm}{\sqrt{6.81 + 1}} = 15.68\ cm$$

$$d = \sqrt{\frac{\lambda^2}{4} + z\lambda} = \sqrt{\frac{(2.75cm)^2}{4} + 20cm \cdot 2.75cm} = 7.54\ cm$$

$$d = 4z\sqrt{\frac{ln2}{(2 + \alpha z)}} = 4 \cdot 20cm \sqrt{\frac{0.69314718}{(2 + 376.73\ \frac{\frac{1}{300}}{2\sqrt{6.81}} \cdot 20cm)}} = 8.14\ cm$$

The diameters calculated above, are representing the footprint of the antenna at a certain distance, every reflector within fully covered by this footprint, won't be recognizable. The footprint effect, also means that the reflector will be visible before the antenna is right above it. Knowing that, we can assume that with a narrower sampling interval, the reflector will reflect before than with a wider sampling interval, as the variation of the distance is lower.

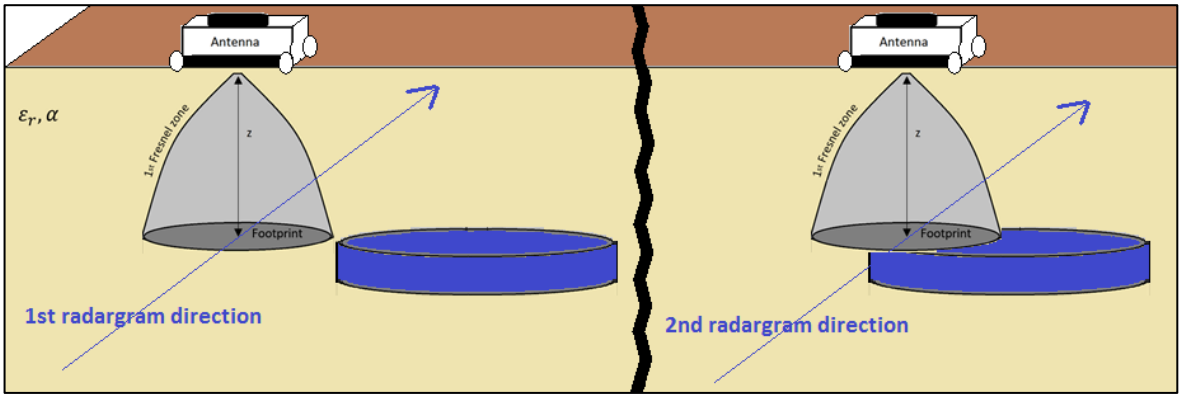

Fig. 8.1. Basic scheme to illustrate the footprint effect when acquiring data.

If we take into consideration the smallest footprint (in this case d=7.54 cm), will cause that our antenna will detect the reflector when it is positioned at a distance equal to the radius of the footprint (r=3.77

cm) to the reflector. Us having our first sampling interval set at 1 cm, that means that at least, the antenna will detect the reflector almost 4 samples before the antenna is actually above the reflector and that causing over-reflection of the object. That over-reflection summed to the fact that the reflector is wider than our footprint, is translated to a deformation on the final shape of the 3D representation of the object. If we add to this, the fact that it may be non-desired reflections around the studied object such: as accumulation of air due to a heterogeneous bury, rocks and other reflectors existent on the ground or spread corrosion from the metal reflector around it; the deformation of the 3D volume is even greater.

Following strictly the same filtering and rendering processes for different sampling intervals. We have done 3D volume representations with sampling interval of 1cm, 2cm, 3cm, 4cm and 5cm. For every sampling interval, is there is the same number of combinations as centimeters are, that is, for 1cm sampling interval there will be 1 combination, for 2cm, sampling interval there will be 2 combinations and so on.

On the following images, you can see that the 3D volumes shape are very reliant on which radargrams are chosen to create the mentioned 3D volumes. However, the best representation of the cylinder, is the one with the sampling interval of 2cm, which is the most closest to the sampling interval calculated by the Niquist-Shanon therorem.

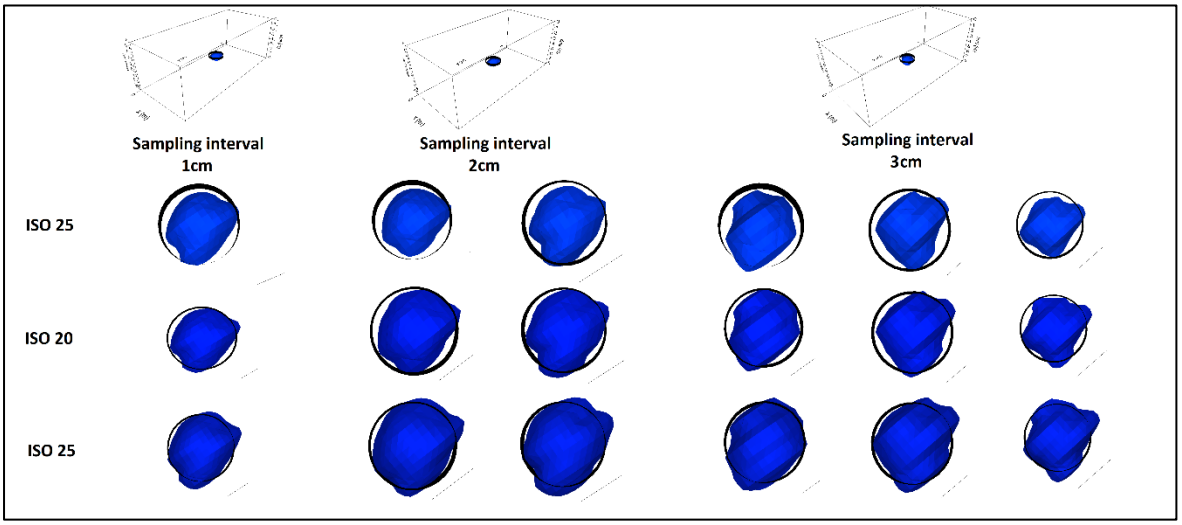

Fig. 8.2. Representation of the different possibilities when surveying with the different sampling intervals (from 1 to 3cm). Notice that the best resolution is find at a sampling interval of 2cm.

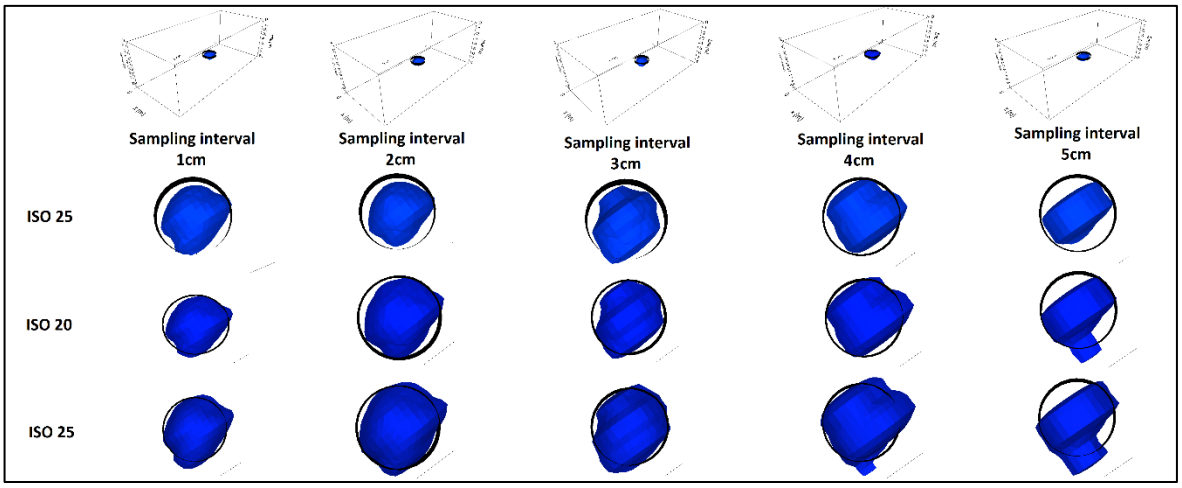

Fig. 8.3. Representation of the different possibilities when surveying with the different sampling intervals (from 1 to 5cm). Notice that only one of the options for each sampling interval is represented. This is to show the fact that a high sampling interval (5cm) makes the 3D volume lose the original shape of the reflector even if the footprint of the antenna is wider than the sampling interval.

From Test 2

What we can extrapolate from this test is that surveying reflectors which are made of different materials affect the 3D representation of them. Survey materials which had a lower reflection than the other aside them, make the 3D volume not visible or barely visible. Specifically, on this test we studied a plastic tube and a solid metallic bar. Processing the 2 objects at the same time, cause the 3D volume of the metal bar to be perfectly visible and recognizable but the plastic pipes appears unrecognizable at all. However, if we only process the part of the radargrams which contains the plastic pipe, the 3D

volume is visible with a pretty acceptable resolution. On the following images you will see the difference of resolution when both tubes are processed at the same time and when the plastic tube is processed alone. Different ISO filters are set on the different images and what ISO setting basically does is that filters a percentage of the amplitudes set; e.g. a 0 ISO will filter 0% of the amplitudes to create the 3D volume, thus the volume will be the whole 3D box because any amplitude will be filtered to create the volume and a 100 ISO will filter all amplitudes, this you won't see anything because all amplitudes where taken out. Remember that he following images are all with the same radargrams and most important, that the radargrams are perpendicular to the pipes.

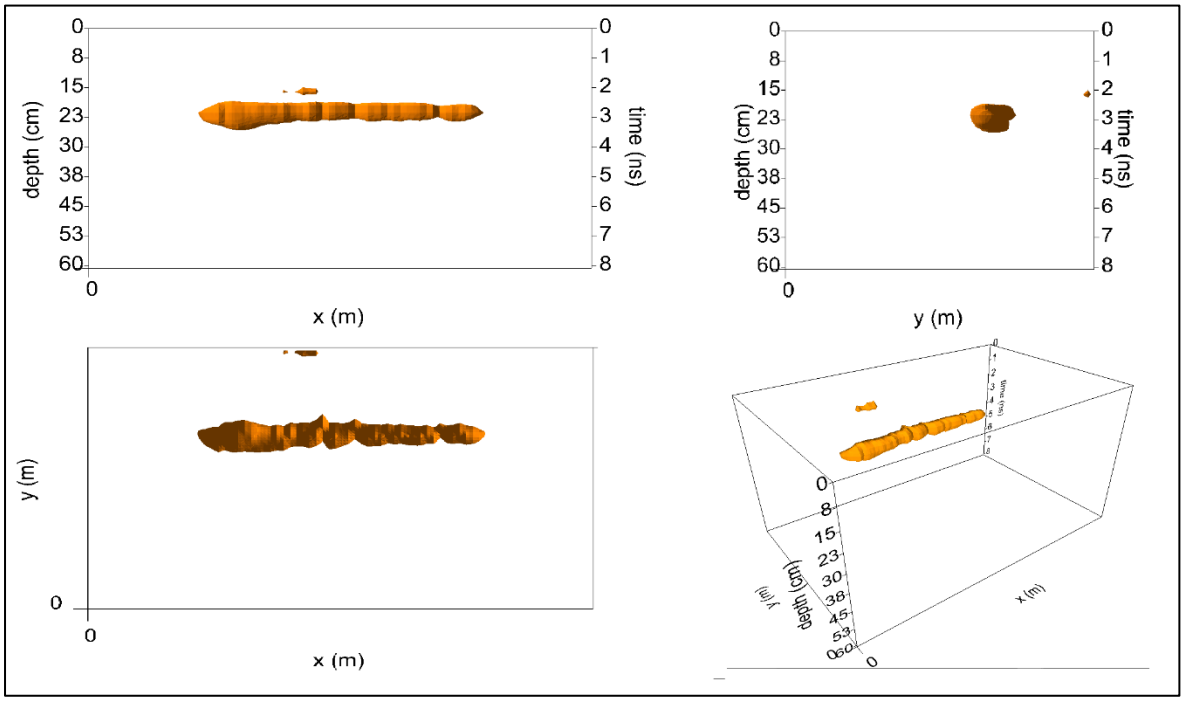

Fig. 8.4. 3D image representation of the metallic bar. Image obtained after a background removal and a migration (relative permittivity 6.81, gain 1) filter. Notice that at this image, the plastic pipe does not appear.

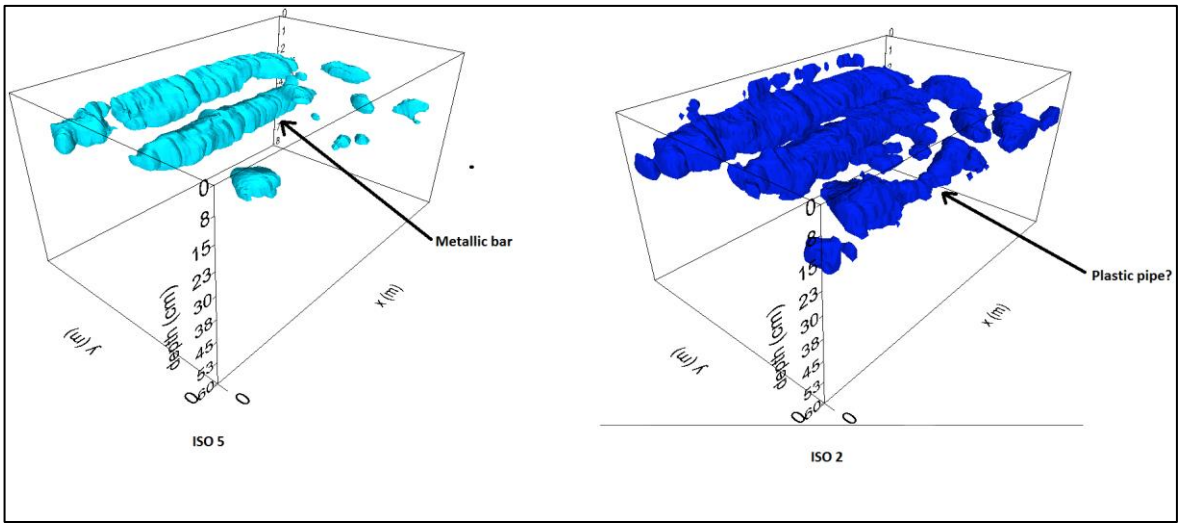

Fig. 8.5. Augment the ISO filter, does not help on representing the plastic pipe, which is "eclipsed" by the metallic bar.

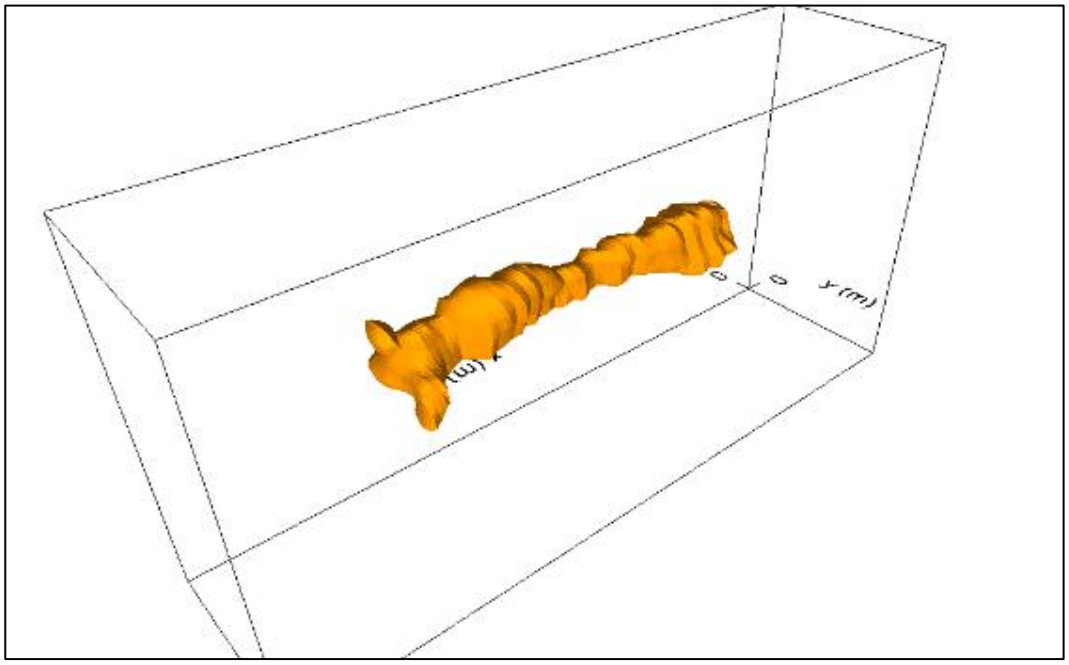

Fig. 8.6. 3D representation of the plastic pipe. Subtracting the metal bar from the total representation, eliminates the "eclipsing" effect, which allows us to represent it properly.

We can observe that the plastic pipe alone as a poorest resolution than the metallic bar. This poorest resolution is due to the fact that the reflection of the plastic is so much lower than the reflection of metal and even more, the permeability of the plastic (one of the parameters which impacts on the reflection) is lower than the permeability of our soil (plastics are around 2 and 5; and the ground in this project has a relative permeability of 6.81). When this is combined with other factors such as the heterogeneity of the medium, the final resolution of the reflector results to be worst.

For this set up (metal bar+plastic pipe) we also performed the study with the direction of the radargrams parallel to the pipes. In this case, we can observe a very revealing result, which is, that the resolution of the final 3D volume are pretty awful performing the same processing as the other studies.

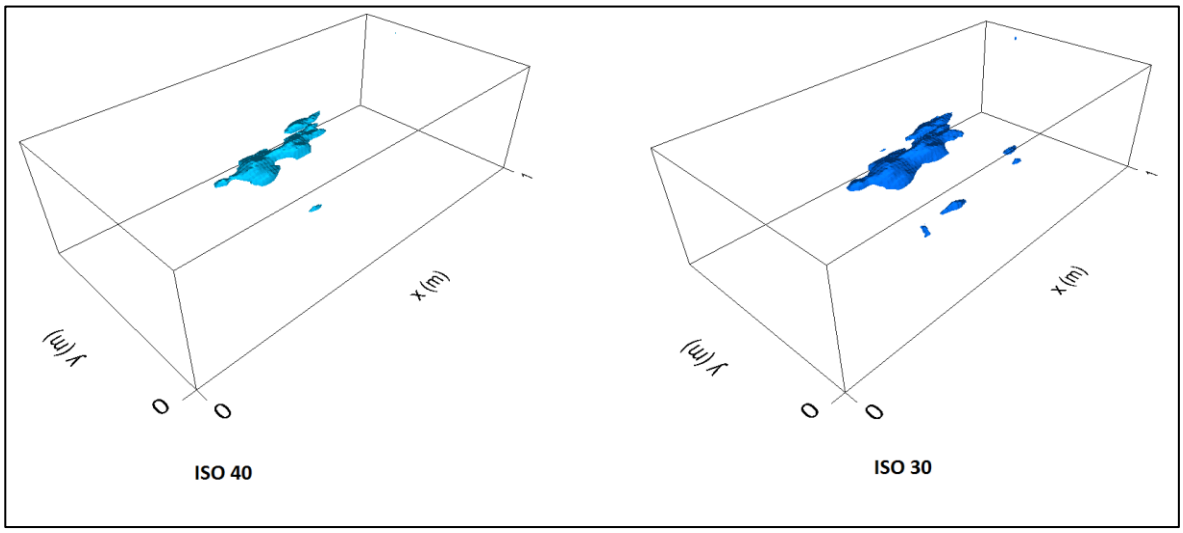

Fig. 8.7. 3D representation of the tubes. Notice that again, only the metal bar is show. However, the resolution is awful due to the direction of the radargrams.

As you can see, just the metallic bar volume is most likely to left it to interpretation rather than really observe and distinguish a bar. This is so important because it literally tells us that the direction of the radargram has huge importance when it comes to interpret data making it more difficult depending on how we approach the survey.

From Test 3

From test of 3 metallic plates at different depths we can conclude with a sentence: in order to create a 3D volume of different reflectors at different depths, it is needed to adjust the gain in order that the targets that are deeper had more gain than the ones near to the surface. Due to absorption and scattering effects, deeper located targets reflect smaller amplitudes than objects nearer to the surface and cause that when representing all objects in the same volume, deeper ones are more difficult to differentiate. In this test, can also appreciate the importance of the direction of the radargrams, here radargrams where take parallel to the dominant direction of the plates and thus, the dimension of the volumes unreal, being the issue a deformation on the normal axis of the direction of the radargrams produced by the footprint effect which makes that GPR detects the reflection when it is not above it.

Fig. 8.8. Metal plates placement

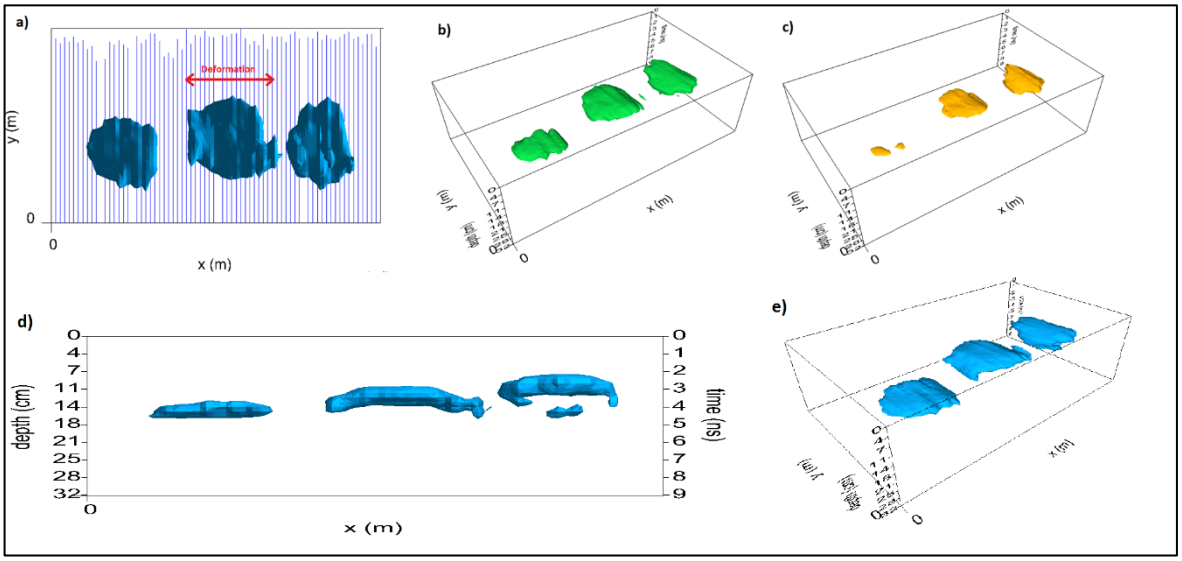

Fig. 8.9. Notice the deformation perpendicular to the direction of the radargrams on image a), the proper height representation on d) and e); and see how changing the iso on b) and c) produces that the deeper plate is almost erased from the representation.

From Test 4

Unfortunately, test 4 was the most difficult test to process and interpret to the point that almost nothing substantial can be represented either in 2 or 3D. However, this not necessary a bad thing because some information can be drawn from this "failure". First off, the impossibility to create a 3D valid volume confirms what we conclude from test 2: different materials (with very contrasting electromagnetic properties) at same depth and in the same volume are so difficult to represent in 3D. The 4 objects where made of distinct materials: a wax sphere, a hammer with a wood handle and a rubber head, a metallic cylinder (the same we used in test 1) and a metallic plate (same we used in test 3).

In addition, this result also help us to understand the implications of salt in the soil. High salinity increments the permittivity of the soil which makes more difficult for insulators to reflect properly.

From all tests

A common effect seen on all tests is regarding a significant deformation of the 3D volumes in the direction of movement of the antenna. That is, that the final volumes are stretched and deformed on the direction of movement which can be caused most probably by the shape of the antenna footprint. As we explained on chapter "Horizontal Resolution", the footprint of the antenna is not a perfect circle but is most likely like an ellipse with the focus points virtually located depending on the position of the transmitter bow tie conductor. Our antenna (MALA 1.6MHz) has the bow ties positioned as is shown in the image (Fig. 4.2) so the focus of the footprint ellipse are located just like in the image (Fig. 8.9.).

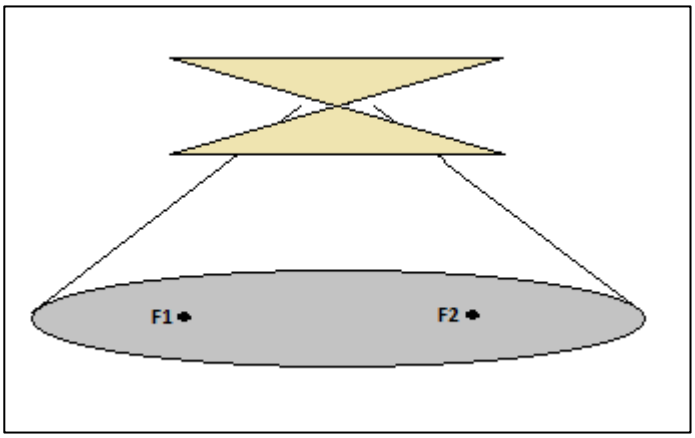

Fig. 8.10. Bow tie of the antenna with the footprint ellipse scheme

Overall

The aim of this project was to set some recommendations/rules to optimize 3D images from GPR radargrams based on experimental surveys with controlled conditions.

- Radargrams gain play a very important role on a volume representation since with GPR-Slice volumes are created based on amplitude changes and depending how the operation manages the radargram gains is critical to obtain 3D volumes with a good resolution. Deeper reflector will need higher gain if the operator wants to represent objects at different depths in order to even amplitudes against depth.
- The direction in which the radargrams are taken is also a critical matter, because radargrams are a representation of the reflection of discontinuities on the ground and even if a radargram is a 2D representation, the transition and reflection has a 3D nature. With that in mind, radargrams not only a representation of amplitude changes in depth but also in horizontal distance and in some way, even if the antenna is not right above the reflector, radargrams will capture part of it. Then, how to manage the direction? When the user wants to represent an object that one its dimensions is dominating upon the others (typically 1/10 or less), such as beans, bars, columns, roots, walls, etc., the recommendation is to manage the direction to be perpendicular to dominant dimension of the desired object. For example if a beam has it longest dimension pointing to the X axis, the GPR radargrams should be taken pointing to the Y axis to have an optimal 3D representation.
- Different materials, and more specifically, different materials with very differentiated electromagnetic properties, should be represented in different 3D volumes, because the higher the reflection of one of the objects is compared to the other, the more difficult will be to represent in 3D the both objects at the same time, being very difficult to represent the object with lower reflections.
- Volumes turn out to stretch in the direction of the acquirement of the radargrams. Is not a major deformation, but is something to take into consideration when the final volume is represented
- Dense gridding and a high number of slices is a must. It can be logical but it is necessary to mention that if the operator desires high resolution 3D volume representation, a high number of radargrams per square meter is needed. In the same way, the more slices obtained from radargrams the better the depth resolution will be. For dense gridding follow the theory of Niquist-Shanon theorem applied to samplings intervals which basically says that to have a dense gridding, the sampling interval should be a quarter of the wavelength. We don't recommend, though, to survey with a very small sampling interval for two main reasons: time (more radargrams means more time) and possible deformations due to over-sample the soil.

Future working lines

Drawn from this project, there have opened lot of possibilities that should be very interesting to dig in. The following list is a bunch of future possible lines of study:

- Expand, improve and build on the tutorial of create 2D time slices in GPR-Slice
- We have noticed an interesting effect when representing in 3D the metallic cylinder: the volume processed by the software presents a bump under the actual volume presumably because of a wave packet after the first total reflection of the metallic object. This effect should be possible to eliminate under different other processing (which we did not performed on this project such) as deconvolution, band pass filters and others.
- Experiment with more and more objects, antennas, equipments, situations, shapes, positions… in order to improve the 3D representation with GPR.

Bibliography

Conyers, Lawrence B. 2016. Ground-Penetrating Radar for Geoarchaeology. West Sussex : Wiley Blackwell. 2016.

Deiana, Daniela. 2008. A Texture Analysis of 3D GPR Images. Delft : Delft University of Technology, 2008. Master Thesis.

Goodman, Dean and Piro, Salvatore. 2013. GPR Remote Sensing in Archaeology. New York : Springer Heidelberg New York Dordrecht London. 2013.

GPR-SLICE V7.0. 2016. Ground Penetrating Radar Imaging Software, User's Manual. California : GPR-SLICE. 2016.

Ingenieurbüro obonic. "Ground Penetrating Radar History". Web: https://www.obonic.de/en/history-ground-penetrating-radar-technology/. (Consulted 20-10-2016)

Institution of Electrical Engineers, The; London, United Kingdom. 2004. Ground Penetrating Radar – 2nd Edition *Edited by Daniels, David J.* Herts : The Institution of Electrical Engineers. 2004.

[Ed.] Jol, Harry. 2008. Ground Penetrating Radar Theory and Applications. Oxford: Elsevier Science. 2008.

Leucci, Giovanni; Negri, Sergio and Carrozzo, Maria Teresa. 2003. Ground Penetrating Radar (GPR): an application for evaluating the state of maintenance of the building coating. Lecce : Università di Lecce. 2003.

MALA GPR. 2012. Main unit for the MALÅ Geoscience High frequency antenna series Operating manual, Version 2.7. Sweden: MALA GPR. 2012.

Novo, Alexandre; Grasmueck, Mark; Viggiano, Dave A. and Lorenzo, Henrique. 2002. 3D GPR in Archeology: What can be gained from dense Data Acquisition and Processing?. 12th International Conference on Ground Penetrating Radar, June 16-19, 2008, Birmingham, UK. ResearchGate, July 2002.

Novo, Alexandre; Lorenzo, Henrique; Rial, Fernando I.; Pereira, Manuel and Solla, Mercedes. 2002. Ultra-dense grid strategies for 3D GPR in Archaeology. 12th International Conference on Ground Penetrating Radar, June 16-19, 2008, Birmingham, UK. ResearchGate, July 2002.

Pérez Gracia, Vega. 2001. *Radar de subsuelo. Evaluación para aplicaciones en arqueología y en patrimono histórico- artístico.* Barcelona: Polytechnic University of Catalonia. Doctoral Thesis. UPC COMMONS, 2001.

Pérez Garcia, Vega. 2010. Resolution in evaluation of structural elements by using ground-penetrating radar. Barcelona : Polytechnic University of Catalonia, 2010.

Pérez Gracia, Vega; González-Drigo, Ramón and Di Capua, Daniel. 2008. Horizontal resolution in a non-destructive shallow GPR survey: An experimental evaluation. Barcelona : Polytechnic University of Catalonia. NDT&E International 41, 2008.

Rial, Fernando I.; Pereira, Manuel; Lorenzo, Henrique; Arias, Pedro and Novo, Alexandre. 2007. Vertical and Horizontal Resolution of GPR bowtie antennas. Natural Resources and Environmental Engineering, University of Vigo. ResearchGate, July 2007. Conference paper.

Rovira Rocasalbas, Yolanda. 2015. *Análisis de una zona del Eixample de Barcelona utilizando la señal debida a la retrodispersión de la onda electromagnética para determinar características geológicas superficiales.* Barcelona : Polytechnic University of Catalonia, 2015. Final bachelor's degree project.

Sensors & Software Inc. 1999. Ground Penetrating Radar Survey Design. Mississagua : Sensors & Software Inc. 1999.

Vera Tapias, Alberto. 2012. *EXPLORANDO LAS ONDAS: UNA PROPUESTA DIDÁCTICA PARA LA ENSEÑANZA - APRENDIZAJE DE ALGUNOS CONCEPTOS BÁSICOS DEL MOVIMIENTO ONDULATORIO.* Bogotá : Universidad Nacional de Colombia, 2012. Master Thesis.

Warren, Craig and Giannopoulos, Antonios. 2010. Creating FDTD models of commercial GPR antennas using Taguchi's optimization method. Scotland : Institute for Infrastructure and Environment School of Engineering. The University of Edinburgh. 2010.

Young, E.J. 2013. Section 1.1.5. Ground Penetrating Radar. In: Robinson, Martin; Bristow, Charlie; McKinley, Jennifer and Ruffell, Alastair (Eds.) Geomorphological Techniques (Online Edition). British Society for Geomorphology; London, UK. ISSN: 2047-0371.